*Pedosphere* doi:10.1016/j.pedsph.2025.04.008
ISSN 1002-0160/CN 32-1315/P

Published by Elsevier B.V. and Science Press

Research Article

# Amorphous and plant-available silicon status of the soils of Lower Austria

Dmytro MONOSHYN[1,2], Mirriam C. CHIBESA[1], Markus PUSCHENREITER[3], Olivier DUBOC[3], Jakob SANTNER[1,4,*], Walter W. WENZEL[3,*]

[1]*BOKU University, Department of Crop Sciences, Institute of Agronomy, Konrad-Lorenz-Strasse 24, Tulln an der Donau 3430 (Austria)*
[2]*BOKU University, Institute of Zoology, Gregor-Mendel-Straße 33/I, Vienna 1180 (Austria)*
[3]*BOKU University, Department of Forest- and Soil Sciences, Institute of Soil Research, Konrad-Lorenz-Strasse 24, Tulln an der Donau 3430 (Austria)*
[4]*Justus Liebig University Giessen, Institute of Plant Nutrition, Heinrich-Buff-Ring 26-32, Giessen, D-35392 (Germany)*

(Received March 10, 2025; revised April 7, 2025; accepted April 11, 2025)

## Abstract

Silicon (Si) is a beneficial element that enhances plant resistance against biotic and abiotic stresses, *e.g.*, drought and fungal infections. Little is known about amorphous and plant-available Si concentrations of agricultural soils of the temperate climate zone and the factors influencing them, as regional studies are scarce. In this study, we analyzed calcareous and non-calcareous topsoils (0-20 cm) from 146 grassland and 271 cropland sites in Lower Austria for amorphous silica (ASi), $CaCl_2$-extractable Si ($Si_{CaCl2}$) and key soil characteristics with the goal to investigate the current status and environmental controls affecting soil Si levels. Using the Random Forest algorithm, we identified carbonate (negatively) and clay content (positively) to be highly associated with the model outputs for soil ASi concentrations ($r^2$ = 0.48, RMSE = 852), and the ASi concentration (positively) and soil pH (positively) to be highly associated with soil $Si_{CaCl2}$ concentrations ($r^2$ = 0.54, RSME = 11.8). Between two soil sampling campaigns (1986-2000, 2015-2020), we observed no significant change in amorphous silica concentrations, but a significant increase in $Si_{CaCl2}$ concentrations in calcareous croplands and in non-calcareous grasslands, likely associated with soil management changes that occurred in the area in this period. Moreover, $Si_{CaCl2}$ was found to be low in many soils compared to potential Si uptake by strong Si accumulator plants. Our findings provide valuable insights into so far scarcely studied controls and long-term dynamics of ASi and $Si_{CaCl2}$ in soils of the temperate zone.

*Key Words*: amorphous silica, available silicon, croplands, grasslands, random forest

**Citation**: Monoshyn D, Chibesa M C., Puschenreiter M, Duboc O, Santner J, Wenzel W W. 2025. Amorphous and plant-available silicon status of the soils of Lower Austria. *Pedosphere*. https://doi.org./10.1016/j.pedsph.2025.04.008.

*Corresponding author. E-mail: walter.wenzel@boku.ac.at, jakob.santner@agrar.uni-giessen.de

# INTRODUCTION

The recognition of the role of silicon (Si) in plant nutrition can be traced back at least to 1804 (Saussure, 1804), and since then, the understanding of the role of Si in plants has strongly developed. Si enhances plant resistance against salinity (Singh *et al.*, 2022), drought (Gong *et al.*, 2003; Johnson *et al.*, 2022), and heavy metal toxicity (Wu *et al.*, 2016), while growth on Si-depleted soils decreases the productivity of tomato (Miyake and Takahashi, 1978), soybean (Miyake and Takahashi, 1985), rice (Savant *et al.*, 1997) and potentially of other crops. Si was shown to be essential for diatoms (Birchall, 1995) and *Equisetum* (Chen and Lewin, 1969) and is considered beneficial for other plant species. The dynamics of Si in the soil-plant system, however, are very complex and not yet understood in detail (Haynes, 2014). While Si is ubiquitous, only a small fraction participates in the biogeochemical cycle (Conley, 2002), and only Si in the form of silicic acid ($H_4SiO_4$), often also termed dissolved Si (DSi), is directly available for plant uptake (Casey *et al.*, 2004). Together with sorbed Si species and easily soluble Si precipitates, silicic acid constitutes the $CaCl_2$-extractable Si fraction ($Si_{CaCl2}$), which is generally well correlated with plant Si concentration (Meirelles *et al.*, 2022), although contrasting observations were also reported (Keeping, 2017). After uptake into plants, silicic acid is deposited in plant tissues as precipitated $SiO_2 \cdot nH_2O$ (*i.e.*, hydrated amorphous silica), a material also referred to as phytoliths or plant opal (Sangster and Hodson, 2007; Sharma *et al.*, 2019). These phytoliths are returned to the soil together with plant litter, and are part of the soil amorphous silica (ASi) pool, which also comprises other biogenic silica forms (*e.g.* from diatoms) and minerogenic ASi (Sauer *et al.*, 2006). The primary soil silicates are the only source of dissolved Si at the initial stages of soil development, but their role in its replenishment decreases with the continuation of soil development and the formation of the ASi pool, which is largely replenished by biological Si cycling (Cornelis and Delvaux, 2016).

So far, the soil Si status was primarily studied in tropical soils, as the combination of high Si accumulation by rice (Ma and Yamaji, 2006) and sugarcane (Meirelles *et al.*, 2022), agricultural practices promoting Si leaching (Nguyen *et al.*, 2016), reduced phytolith recycling (Darmawan *et al.*, 2006), and highly weathered, low-Si soils, create concerns for rice and sugarcane production. Contrary to the tropics, the number of regional studies investigating changes in $Si_{CaCl2}$ concentrations in agricultural soils of the temperate climate region is limited. However, the few available studies report an increase in $Si_{CaCl2}$ associated with soil management practices like liming and crop straw recycling (Caubet *et al.*, 2020; Puppe *et al.*, 2021).

In view of the increasing climatic extremes that are challenging the European agricultural sector, the crop Si supply gains more interest (Bindi and Olesen, 2011; Johnson *et al.*, 2018; Bokor *et al.*, 2021; Iglesias and Garrote, 2015), as Si is known to alleviate abiotic and biotic stress in crops, thereby contributing to yield stability (Gong *et al.*, 2003; Johnson *et al.*, 2022). While the importance of Si in agriculture is increasingly recognized, and the factors influencing its availability are generally understood, there is a lack of comprehensive regional survey studies on this topic. Caubet *et al.* (2020) used a Random Forest algorithm to study $Si_{CaCl2}$ in ~2000 soil sampling sites, using topsoil samples (0-30 cm) covering 6 parent material categories and cultivated and non-cultivated sites. Their study showed that $Si_{CaCl2}$ concentrations are positively correlated with soil pH, clay content, soil organic carbon (SOC), and iron oxide content, and reported the parent material to be one of the most important factors determining soil $Si_{CaCl2}$ concentrations. They explained the positive impact of pH on $Si_{CaCl2}$ by an increase in ASi dissolution with an increase in pH, of clay by its dissolution and the adsorption of Si to clay minerals. Yanai *et al.* (2016) found available Si (determined using the phosphate buffer and acetate buffer extraction methods) to be positively correlated with pH, clay content, amorphous minerals, and crystalline iron (Fe) and (Al) oxides. They explained the correlation with pH by an increase in the adsorption of orthosilicate to soil minerals with increasing pH, and with increasing clay, amorphous and crystalline mineral content by the dissolution of these minerals. Using multiple regression analysis, they were able to explain 65-69% of the variability in available Si with these parameters. Quigley *et al.* (2017) found precipitation, sand content, and soil pH explaining about 74% variation in soil $Si_{CaCl2}$ and 19% in soil ASi concentrations. The negative correlation with precipitation was attributed to higher $Si_{CaCl2}$ plant uptake combined with a higher rate of ASi dissolution and $Si_{CaCl2}$ leaching with increasing precipitation. Increasing soil sand contents impacted soil Si status negatively by increasing leaching rates. The role of pH was attributed to an increase in ASi dissolution.

While these studies provided valuable insights into the dynamics of Si in soil, the authors emphasized that their results are soil-specific and generalization to other regions, soil types, and soil management practices should be done carefully. Thus, although it is generally understood that both climate and soil characteristics are important factors of soil Si dynamics, more regional studies are required to understand the behavior of Si in soils with different characteristics and under different land use.

The limited number of available regional studies on soil ASi and $Si_{CaCl2}$ status and their correlations with other environmental parameters and different agricultural soil management practices represents a considerable gap in the current understanding of soil ASi and $Si_{CaCl2}$ dynamics. Therefore, this study is aimed at

(1) determining which parameters (pH, soil carbonate content, Al and Fe oxyhydroxides content, SOC content, clay content, mean annual precipitation) correlate with ASi and $Si_{CaCl2}$ concentrations in grassland and cropland soils, and at

(2) investigating changes of soil ASi and $Si_{CaCl2}$ concentrations between two soil sampling campaigns in the periods 1986-2000 and 2015-2020 using a large set of 417 soil samples from the Austrian province of Lower Austria.

## MATERIALS AND METHODS

### *Soil sampling*

The soils were initially sampled and characterized for the purpose of soil mapping in the period 1986-2000 (initial sampling, 'IS'). We retrieved locations and original soil data from the Austrian Digital Soil Map (BFW, 2023; https://bodenkarte.at/) for regions of the province of Lower Austria (Niederösterreich) for which archived soil samples of the initial sampling campaign were available (Fig. S1, see Supplementary Material for Fig. S1). In the years 2015-2020 we revisited these sites and collected at least 10 topsoil subsamples per site from the same depth as in the original campaign (A horizon). The subsamples were distributed randomly within a circle of 10 m diameter around the initial sampling location and combined to obtain a composite sample (resampling, 'RS'). Note that the accuracy of the comparison with the initial sample may be limited by the spatial variability of soil properties within each sampling site. Therefore, we can only compare mean values of the whole dataset and of subcategories with sufficient sample size (*i.e.*, according to land use or carbonate content).

Of the 569 soils collected, 417 were used for this study: 271 from cropland and 146 from grassland sites. Only the soils from the sites where no changes in the land use occurred between the sampling campaigns, *i.e.* with continuous use as arable land or grassland, were included in this study. The major soil groups (IUSS 2022) in the study region include Phaeozems, Chernozems, Cambisols, Gleysols, Umbrisols, Regosols, and Fluvisols.

The samples were air-dried and sieved to <2 mm. In addition to their land use (arable/grassland), the sites were split into calcareous (≥5 g $kg^{-1}$ $CaCO_3$ equivalent) and non-calcareous (<5 g $kg^{-1}$ $CaCO_3$ equivalent) groups as we expected $CaCO_3$ content to have a key role in ASi accumulation in soil. A subsample was taken from every sample and milled with a ball mill (Retsch MM 400) for the analyses that required finely homogenized soil.

### *Soil analysis*

Information about soil organic matter, total carbonate content, pH, and texture of the soils, analyzed during the initial sampling campaign, was retrieved from the Austrian Digital Soil Map (eBOD) information system (BFW, 2023). The data provided by eBOD is based on methods as follows: to determine textural classes (sand (2000–63 µm), silt (63–2 µm), and clay (<2 µm)), samples were dispersed with sodium pyrophosphate and, at soil organic carbon (SOC) content >50 g $kg^{-1}$ pre-treated with $H_2O_2$ prior to the application of sieving and sedimentation analysis. Soil carbonate content was measured using the Scheibler calcimeter (ÖNORM L 1084, 1989), total organic carbon content was analyzed by dry combustion (ÖNORM L 1080, 2013) using a Vario Macro Cube (Elementar, Germany).

Soil organic carbon was calculated as the difference between the total and inorganic carbon. Soil pH was measured in a solution of 0.01 mol $L^{-1}$ $CaCl_2$ at a soil:solution ratio of 1:2.5. It was assumed that soil texture was stable in the period from IS to RS, so this parameter was not remeasured in the RS samples.

The amorphous oxyhydroxides of Al and Fe (AlOx and FeOx) were measured by a modified Loeppert and Inskeep (1996) procedure (Wenzel *et al.*, 2023) in IS samples only. The filtrate was acidified by the same volume of 4 % $HNO_3$ and stored at 4 °C. For measuring Al (averaged wavelengths 308.215–396.153) and Fe (238.204–239.562) using ICP-OES (OPTIMA 8300, Perkin Elmer, Rodgau-Jügesheim, Germany), we added 1 mL of Yttrium dissolved in 2 % $HNO_3$ as an internal standard to the vials containing 10 mL of the acidified filtrate.

$Si_{CaCl2}$ was extracted using the slightly modified method described by Haysom and Chapman, (1975). Briefly, 3 g of air-dried soil ≤2 mm was placed into a 50 mL plastic vial. 30 mL of 0.01 mol $L^{-1}$ $CaCl_2$ were added. The vials were shaken on an overhead shaker (5 rpm) for 16 hours. Extracts were filtered using plastic funnels and filter paper. Then, the filtrates were analyzed for Si using the colorimetric method (Morrison and Wilson, 1963) on a Varian DMS 200 UV spectrophotometer. Each soil sample was analyzed in duplicate. The only modification made to the original method was the use of 3 grams of soil and 30 mL of $CaCl_2$ solution instead of 2 grams and 20 mL.

Amorphous Si (ASi) was extracted as described by Georgiadis *et al.* (2015). 75 mg of finely milled soil were placed into a 50 mL plastic vial. Thereafter, 30 mL of 0.2 mol $L^{-1}$ NaOH were added, and the vials were shaken on an overhead shaker (5 rpm) for 120 hours at the standard temperature of our laboratory (20-23 °C). After that, the extracts were filtered using plastic funnels and filter paper and analyzed for Si using the colorimetric method (Morrison and Wilson, 1963) on a Varian DMS 200 UV spectrophotometer. This method is well established, and according to Georgiadis *et al.* (2015), only minor amounts of Si from clay minerals and other sources are extracted from temperate-zone soils. Each soil sample was analyzed in duplicate. An overview on the distribution of soil parameter values is given in Table I, an overview on the measurement of parameters in the IS/RS datasets and their use for the data evaluation tasks is given in Table S1 (see Supplementary Material for Table S1) in the Supplementary Information

TABLE I
Overview of soil characteristics of the initial sampling campaign (IS) dataset.

| Land use category | Percentile | pH | ASi | $Si_{CaCl2}$ | AlOx | FeOx | Clay | $CaCO_3$ | SOC | MAP |
|---|---|---|---|---|---|---|---|---|---|---|
| | | | mg $kg^{-1}$ | mg $kg^{-1}$ | mg $kg^{-1}$ | mg $kg^{-1}$ | g $kg^{-1}$ | g $kg^{-1}$ | g $kg^{-1}$ | mm |
| Non-calcareous grasslands | Min | 4.1 | 667 | 2.5 | 691 | 1270 | 70 | 0 | 15.1 | 707 |
| | 0.25 | 5 | 1690 | 7.75 | 1230 | 3260 | 160 | 0 | 27.9 | 1040 |
| | 0.5 | 5.6 | 2290 | 11.1 | 1620 | 4310 | 230 | 0 | 35.2 | 1220 |
| | 0.75 | 6.15 | 3330 | 18.6 | 2120 | 5790 | 290 | 0 | 47.1 | 1460 |
| n = 103 | Max | 7 | 6500 | 40.5 | 4280 | 8980 | 450 | 4.0 | 131 | 1700 |
| Calcareous grasslands | Min | 6.7 | 200 | 4.30 | 156 | 656 | 20.0 | 7.0 | 17.9 | 568 |
| | 0.25 | 7.0 | 706 | 12.0 | 976 | 1580 | 135 | 91.0 | 40.9 | 1070 |
| | 0.5 | 7.2 | 1270 | 18.4 | 1230 | 2260 | 180 | 183 | 52.8 | 1170 |
| | 0.75 | 7.3 | 1850 | 30.1 | 1520 | 2810 | 265 | 384 | 75.5 | 1290 |
| n = 43 | Max | 7.8 | 3680 | 55.2 | 3430 | 6160 | 420 | 540 | 143 | 1530 |
| Non-calcareous croplands | Min | 4.2 | 755 | 1.9 | 284 | 465 | 30 | 0 | 4.1 | 474 |
| | 0.25 | 5.8 | 1931 | 22.5 | 605 | 988 | 170 | 0 | 11.9 | 483 |
| | 0.5 | 6.5 | 2600 | 40.3 | 734 | 1190 | 220 | 0 | 15.7 | 500 |
| | 0.75 | 7.0 | 3520 | 51.0 | 867 | 1900 | 310 | 0 | 22.2 | 581 |

| | | | | | | | | | | |
|---|---|---|---|---|---|---|---|---|---|---|
| n = 99 | Max | 7.4 | 6390 | 96.7 | 1790 | 7150 | 540 | 5.0 | 51.9 | 1088 |
| Calcareous croplands n = 172 | Min | 7.0 | 142 | 5.4 | 102 | 191 | 20 | 6.0 | 5.0 | 474 |
| | 0.25 | 7.4 | 1310 | 24.8 | 663 | 759 | 210 | 31.0 | 15.5 | 489 |
| | 0.5 | 7.5 | 1930 | 33.3 | 847 | 988 | 270 | 105 | 21.6 | 548 |
| | 0.75 | 7.6 | 2540 | 44.4 | 1090 | 1340 | 330 | 234 | 31.5 | 567 |
| | Max | 8.1 | 8960 | 110 | 3110 | 5410 | 620 | 820 | 187 | 959 |

Data summary for the initial sampling (IS) dataset, number of samples = 417. ASi and $Si_{CaCl2}$ are amorphous and $CaCl_2$-extractable Si, respectively. AlOx and FeOx are acid ammonium oxalate extractable Al and Fe, respectively. SOC is soil organic carbon, MAP is mean annual precipitation.

### *Climate data acquisition*

Climate data (precipitation) was obtained from the SPARTACUS dataset (Hiebl and Frei, 2018), which was provided by the Institute of Meteorology, University of Natural Resources and Life Sciences Vienna.

### *Data processing and analysis*

We used a random forest (RF) model (Breiman, 2001) to determine relationships between ASi, $Si_{CaCl2}$ and environmental parameters in the IS dataset (Table I). This model was chosen based on the characteristics of our dataset (high number of variables, clustered nature of sampling sites, possible autocorrelations, categorical variables), limiting the applicability of multiple linear regression. Like many machine learning models, Random Forests (RF) rely on the quality of the training data and typically need a substantial number of observations. However, the impact of the training data's quality can be reduced by using cross-validation. The number of samples in this study was sufficient, and the interpretation was simplified by employing Shapley Additive Explanations (SHAP), which are described below. The RF model is based on classification and regression trees. The model uses bootstrapped sampling on training data to create decision trees. An additional degree of randomness is introduced by taking a random set of predictors (features or factors, referred to as 'explanatory variables' in this work) to generate each tree. The model works with both categorical (after encoding) and numerical predictors, can cover non-linear relationships, and is not sensitive to outliers. The RF model output includes both a prediction (*i.e.* ASi or $Si_{CaCl2}$ concentration predicted for a set of explanatory variables) and the proportional importance of each explanatory variable, referred to as 'variable importance', enabling the analysis of the impact of each variable on the prediction. While the model is commonly used for classification problems, it is applicable to regression problems as well. In this study, 80% of the dataset were used for model training and 20% for testing. This proportion was chosen as it is the most commonly used one (Gholamy *et al.*, 2018; Joseph, 2022).

Python (version 3.8.10) with the packages Pandas (McKinney, 2010), Numpy (Harris *et al.*, 2020), Matplotlib (Hunter, 2007), and Scikit-learn (Pedregosa *et al.*, 2011) was used for data processing, plotting, and modeling.

The Python version of the Boruta package (Kursa and Rudnicki, 2010) was used to reduce the number of variables by removing those with no impact on the RF model output. Boruta creates so-called shadow variables by copying and shuffling the original variables, trains the RF, and evaluates the importance of each variable by measuring the 'mean decrease accuracy' (Bénard *et al.*, 2022), which is a metric to measure the decrease in model accuracy when a specific predictor variable is shuffled. If, as a result of 100 iterations of the RF, the shadow variable has a higher or equal z-score as the corresponding original variable, the original variable is marked as unimportant and excluded from the modeling process.

Five-fold cross-validation (CV) was used to evaluate the performance of the model. The dataset was split into 5 randomly generated partially overlapping subsets (folds) of approximately equal size. Four subsets were used for training and the $5^{th}$ for testing. The procedure was repeated 5 times, each

time using different subsets for training and testing. Model performance was calculated and reported as an average $r^2$ and relative mean square error (RMSE) between folds. Shapley additive explanations (SHAP) values were calculated and plotted as beeswarm plots based on the whole dataset using the SHAP module (see Lundberg and Lee (2017) for further details about SHAP). Beeswarm plots display the impact of features in a dataset on the output of a model. Each dot in a plot represents a single instance (datapoint) of a variable (y-axis) in a dataset, where red represents instances with high and blue with low absolute value of said variable. These plots show the importance of each explanatory variable in the model and the direction and linearity of its impact.

The RF analysis was performed sequentially. ASi was analyzed before $Si_{CaCl2}$, with the 3 parameters showing the highest correlation with ASi being excluded from the $Si_{CaCl2}$ analysis to minimize autocorrelations. The parameter 'land use type' was excluded from the modeling process because of its high degree of correlation with precipitation and thus with site location and topography. Soil group and soil parent material were initially tested as explanatory variables but later excluded from the modeling due to the absence of observed impact.

After the RF analysis, each variable found to be important by Boruta, was plotted individually against ASi or $Si_{CaCl2}$ for each land-use category to evaluate its individual contribution. Therefore, product-moment (Pearson) correlation analysis was carried out, with correlations being regarded significant for $\alpha \leq 0.05$.

### *Changes in soil si status between sampling campaigns*

Our set of samples allowed for an analysis of potential changes in the soil Si status between sampling campaigns, *i.e.* within 20-30 years. We interpret such potential short-term changes in terms of agricultural land management changes, but not in a soil-development perspective, as this short observation period is very unlikely to result in measurable changes caused by soil development. For this analysis, the dataset was split into four subsets based on the land use (cropland *vs.* grassland) and $CaCO_3$ equivalent (calcareous *vs.* non-calcareous soils). All soils with $CaCO_3$ equivalent of >5 g $kg^{-1}$ were categorized as calcareous, and those with $CaCO_3$ equivalent of ≤5 g $kg^{-1}$ as non-calcareous. Using the SciPy package (Virtanen *et al.*, 2020), we employed a two-tailed non-paired t-test with $\alpha \leq 0.05$ to determine whether the differences in ASi and $Si_{CaCl2}$ concentrations were significant between the sampling campaigns and the land use categories (croplands, grasslands), respectively.

## RESULTS

### *The concentrations of asi and $si_{cacl2}$ in soils*

The distribution of ASi and $Si_{CaCl2}$ in calcareous and non-calcareous soils of the second sampling campaign (RS) for the two land use categories is shown in Fig. 1. In contrast to the data compiled in Table I, Fig. 1 represents the current Si status (resampling campaign). Overall, both Si fractions were larger in croplands as compared to grasslands. The ASi concentrations ranged between 86 mg $kg^{-1}$ and 12300 mg $kg^{-1}$, with the following distribution between land use categories (minimum, median, maximum): calcareous croplands: 155, 2010, 5870 mg $kg^{-1}$; non-calcareous croplands: 797, 2700, 12300 mg $kg^{-1}$, calcareous grasslands: 86, 1300, 3890 mg $kg^{-1}$, non-calcareous grasslands: 647, 2150, 5830 mg $kg^{-1}$.

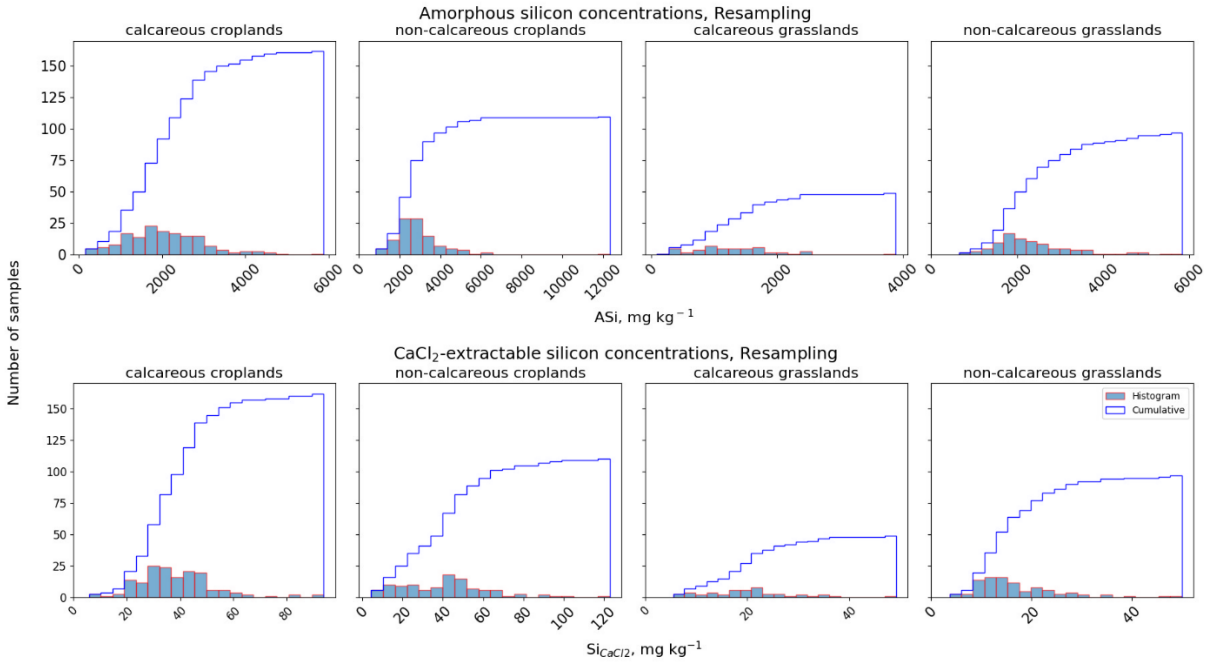


Fig. 1 Distribution of ASi and $Si_{CaCl2}$ concentrations in the soil samples of the resampling campaign. Calcareous croplands: 172 samples, non-calcareous croplands: 99 samples, calcareous grasslands: 43 samples, non-calcareous grasslands: 103 samples.

The $Si_{CaCl2}$ concentrations varied between 3.7 mg $kg^{-1}$ and 122 mg $kg^{-1}$, with the following distribution between land use categories (minimum, median, maximum ): calcareous croplands: 5.9, 36.6, 93.9 mg $kg^{-1}$; non-calcareous croplands: 4.3, 41.6, 123 mg $kg^{-1}$, calcareous grasslands: 5.5, 20.3, 49.2 mg $kg^{-1}$, non-calcareous grasslands: 3.7, 14.8, 50.0 mg $kg^{-1}$ (Fig. 1).

Table II compiles the arithmetic means, medians and standard deviations of ASi and $Si_{CaCl2}$ concentrations in the main soil groups (IUSS Working Group WRB, 2022) of the resampled calcareous and non-calcareous soils beneath cropland and grassland. Generally, the variation of ASi between soil groups is smaller than among calcareous and non-calcareous soils within each land use category, and between land use categories (Table II). The most striking difference between soil groups relates to clearly smaller ASi concentrations of Gleysols and Fluvisols. Similarly, we found smaller variation of $Si_{CaCl2}$ among soil groups compared to that between land use categories.

TABLE II

Amorphous silica (ASi) and $CaCl_2$-extractable silicon ($Si_{CaCl2}$) in topsoils (A horizons) of the main soil groups (IUSS Working Group WRB, 2022) for each land-use category, detailed for non-calcareous and calcareous soils of the resampling campaign. StD indicates standard deviation of the mean. The category 'Others' includes all soil groups with <5 observations.

| Land use category | Soil group | Observation number | ASi | | $Si_{CaCl2}$ | |
|---|---|---|---|---|---|---|
| | | | Median | Mean ± StD | Median | Mean ± StD |
| | | | mg $kg^{-1}$ | mg $kg^{-1}$ | mg $kg^{-1}$ | mg $kg^{-1}$ |
| Non-calcareous grasslands | Cambisol | 51 | 2100 | 2370 ± 1010 | 14.8 | 16.7 ± 7.80 |
| | Regosol | 12 | 2406 | 2400 ± 762 | 14.5 | 17.1 ± 11.2 |
| | Stagnosol | 11 | 2090 | 2370 ± 1090 | 18.7 | 19.8 ± 9.36 |
| | Phaeozem | 9 | 2130 | 2010 ± 605 | 21.8 | 19.6 ± 4.64 |
| | Gleysol | 9 | 1830 | 2280 ± 1450 | 23.2 | 22.9 ± 10.6 |
| | Others | 11 | | | | |
| Calcareous grasslands | Phaeozem | 18 | 1060 | 1190 ± 545 | 18.9 | 18.3 ± 6.72 |
| | Cambisol | 8 | 2450 | 2350 ± 860 | 20.3 | 19.6 ± 6.85 |
| | Regosol | 7 | 1180 | 1220 ± 450 | 21.8 | 21.1 ± 8.25 |

| | | | | | | |
|---|---|---|---|---|---|---|
| | Gleysol | 7 | 791 | 1060 ± 858 | 9.9 | 14.6 ± 10.0 |
| | Others | 3 | | | | |
| Non-calcareous croplands | Phaeozem | 45 | 2880 | 3040 ± 1170 | 44.3 | 44.3 ± 16.6 |
| | Cambisol | 18 | 2540 | 2580 ± 882 | 32.7 | 33.6 ± 19.8 |
| | Chernozem | 9 | 3280 | 3570 ± 946 | 53.1 | 60.9 ± 20.5 |
| | Regosol | 9 | 2340 | 2210 ± 835 | 11.5 | 18.1 ± 14.6 |
| | Others | 18 | | | | |
| Calcareous croplands | Phaeozem | 72 | 1980 | 2280 ± 1480 | 38.4 | 40.2 ± 15.1 |
| | Regosol | 38 | 1920 | 2070 ± 1260 | 39.2 | 41.3 ± 20.0 |
| | Chernozem | 24 | 2430 | 2300 ± 948 | 38.1 | 39.2 ± 13.7 |
| | Gleysol | 15 | 1810 | 1920 ± 1160 | 32.7 | 32.4 ± 14.5 |
| | Cambisol | 8 | 1850 | 1920 ± 970 | 36.4 | 36.1 ± 8.2 |
| | Fluvisol | 7 | 1520 | 1560 ± 833 | 30.8 | 30.8 ± 15.2 |
| | Others | 8 | | | | |

*Model performance and variable importance*

The performance of the models for ASi and $Si_{CaCl2}$ was evaluated using 5-fold cross-validation, resulting in a mean $r^2$=0.48 and RMSE of 852 mg $kg^{-1}$ for ASi, and a mean $r^2$=0.54 and RMSE of 11.8 mg $kg^{-1}$ for $Si_{CaCl2}$ as the averages between folds (Table III). See Fig. S2 (see Supplementary Material for Fig. S2) for the $r^2$ and basic model regression plots (no cross-validation averages).

The RF analysis showed that $CaCO_3$ equivalent, clay content, and precipitation had the strongest association with soil ASi concentration (Fig. 2A, B), followed by soil pH and SOC having similar levels of correlation with soil ASi. Among the explanatory variables, $CaCO_3$ equivalent, pH, and SOC are negatively, whereas clay content positively related to ASi. High precipitation was mainly associated with negative impacts on the model output, however, in some instances, the opposite effect was observed (Fig. 2B). AlOx and FeOx were excluded from the ASi model as they were claimed unimportant by the Boruta algorithm.

The RF analysis showed that pH, ASi, and FeOx had the strongest impact on $Si_{CaCl2}$ concentration in soil (Fig. 2C, D), followed by soil organic carbon and AlOx. ASi and pH had a strong positive impact on $Si_{CaCl2}$ with a similar magnitude. FeOx and SOC had a mainly negative impact on the model output: both high and low individual instances were associated with lower $Si_{CaCl2}$, but only the low ones were associated with high $Si_{CaCl2}$. The magnitude of SOC impact was approximately half of that of FeOx. Large AlOx concentrations were always negatively impacting $Si_{CaCl2}$ concentrations, but the magnitude of the effect was small (Fig. 2D). $CaCO_3$ equivalent, clay content, and mean annual precipitation were removed from the model to limit autocorrelations. No variables were claimed unimportant by Boruta.

TABLE III
Random Forest 5-fold cross validation performance.

| ***Dependent variable*** | ***RMSE (mg $kg^{-1}$)*** | ***$r^2$*** | ***Explanatory variables*** | ***Excluded explanatory variables*** |
|---|---|---|---|---|
| ASi | 852 | 0.48 | $CaCO_3$, Clay, Precipitation, SOC, pH | AlOx, FeOx (Boruta) |
| $Si_{CaCl2}$ | 11.8 | 0.54 | ASi, pH, FeOx, SOC, AlOx | $CaCO_3$, Clay, Precipitation (to avoid autocorrelation) |

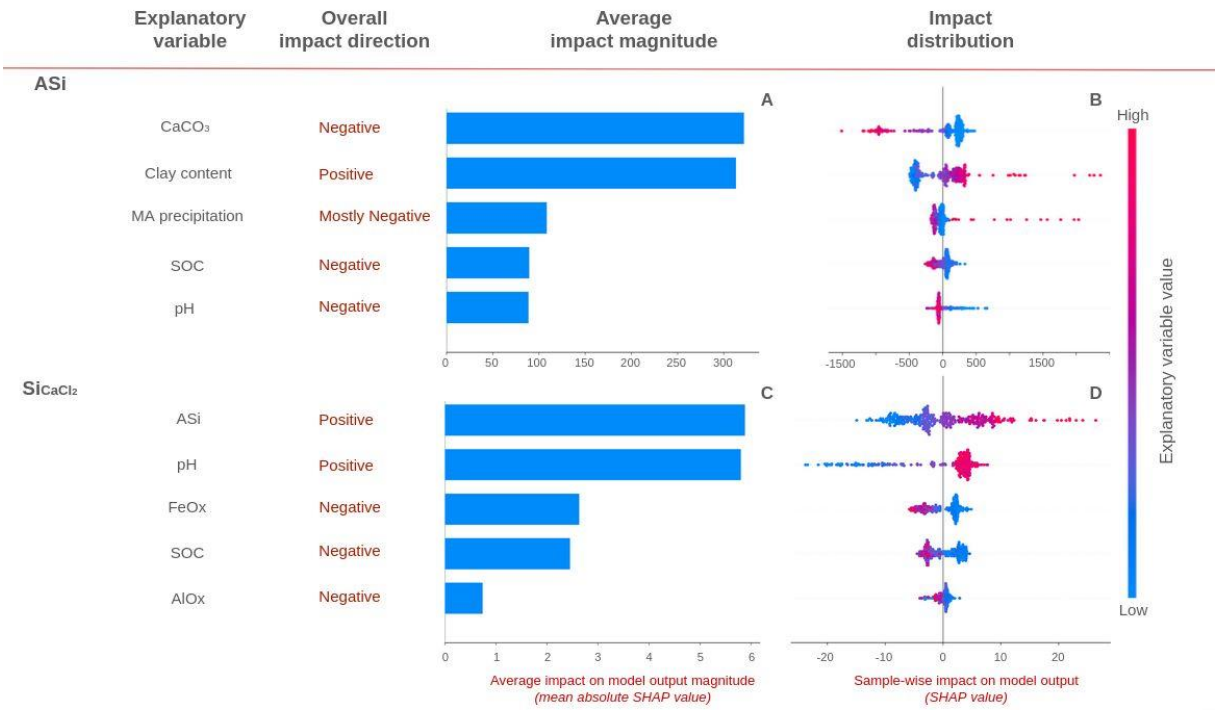


Fig. 2 SHAP summary showing importance and impact of explanatory variables on ASi (A, B) and $Si_{CaCl2}$ (C, D) predictions. Panels A and C show magnitude and direction (positive/negative) of the impact each explanatory variable has on the model output for ASi and $Si_{CaCl2}$, respectively. Panels B and D show the distribution of impact of each explanatory variable on model output for ASi and $Si_{CaCl2}$, respectively, as beeswarm plots. Each point on the beeswarm plots represents an individual sample. Beeswarm color represents the value of explanatory variables, red for high, blue for low. The SHAP value (*X*-axis) represents the impact of the explanatory variable value on model output. MA precipitation: mean annual precipitation, SOC: soil organic carbon, FeOx and AlOx: ammonium-oxalate-extractable iron and aluminum. The SHAP value unit is that of the target variable (*i.e.*, ASi or $Si_{CaCl2}$ in mg $kg^{-1}$ soil). For interpretation of the references to color in the Fig., please refer to the Web version of this article.

## *Analysis of individual correlations between asi, $si_{cacl2}$, and other variables*

In the following, individual correlations of the five most important explanatory variables, according to Table III, are reported for ASi and $Si_{CaCl2}$. Only statistically significant correlations ($p \leq 0.05$) are described in the text. As an additional criterion, we discuss only correlations with $R^2 \geq 0.05$. Therefore, very weak, but significant correlations are considered negligible and not are discussed.

Negative correlations between $CaCO_3$ and ASi concentrations were observed in calcareous croplands (Fig. 3A; $R^2 = 0.28$) and grasslands (Fig. 4A; $R^2 = 0.16$). Positive correlations between clay content and ASi were observed in calcareous croplands (Fig. 3B; $R^2 = 0.23$), non-calcareous croplands (Fig. 3B; $R^2 = 0.56$), and calcareous grasslands (Fig. 4B; $R^2 = 0.24$). Negative correlation between mean annual precipitation and ASi concentrations were observed in non-calcareous ($R^2 = 0.14$) and calcareous ($R^2 = 0.12$) croplands (Fig. 3C), while in non-calcareous grasslands this correlation was positive (Fig. 4C; $R^2 = 0.20$). Negative correlations between SOC and ASi concentrations were observed in calcareous croplands (Fig. 3D; $R_2 = 0.11$) and grasslands (Fig. 4D; $R^2 = 0.20$). Negative correlations between pH and ASi were observed in calcareous croplands (Fig. 3E; $R^2 = 0.07$) and non-calcareous grasslands (Fig. 4E; $R^2=0.35$).

Positive correlations between ASi and $Si_{CaCl2}$ concentrations were observed in calcareous (Fig. 5A; $R^2 = 0.36$) and non-calcareous croplands (Fig. 5A; $R^2 = 0.43$), and calcareous grasslands (Fig. 6A; $R^2 = 0.20$), respectively. This correlation was negative for non-calcareous grasslands (Fig. 6A; $R^2 = 0.08$). Positive correlations between pH and $Si_{CaCl2}$ and were observed for non-calcareous croplands (Fig. 5B; $R^2 = 0.28$) and non-calcareous grasslands (Fig. 6B; $R^2 = 0.40$). This correlation was negative for calcareous croplands (Fig. 5B; $R^2 = 0.06$). The soil FeOx content showed no individual correlations to $Si_{CaCl2}$ in our dataset. A negative correlation between SOC and $Si_{CaCl2}$ was observed in calcareous grasslands (Fig. 6D; $R^2 = 0.13$), while in non-calcareous grasslands (Fig. 6D; $R^2 = 0.11$) this correlation was positive. No individual correlations between $Si_{CaCl2}$ and soil AlOx were found.

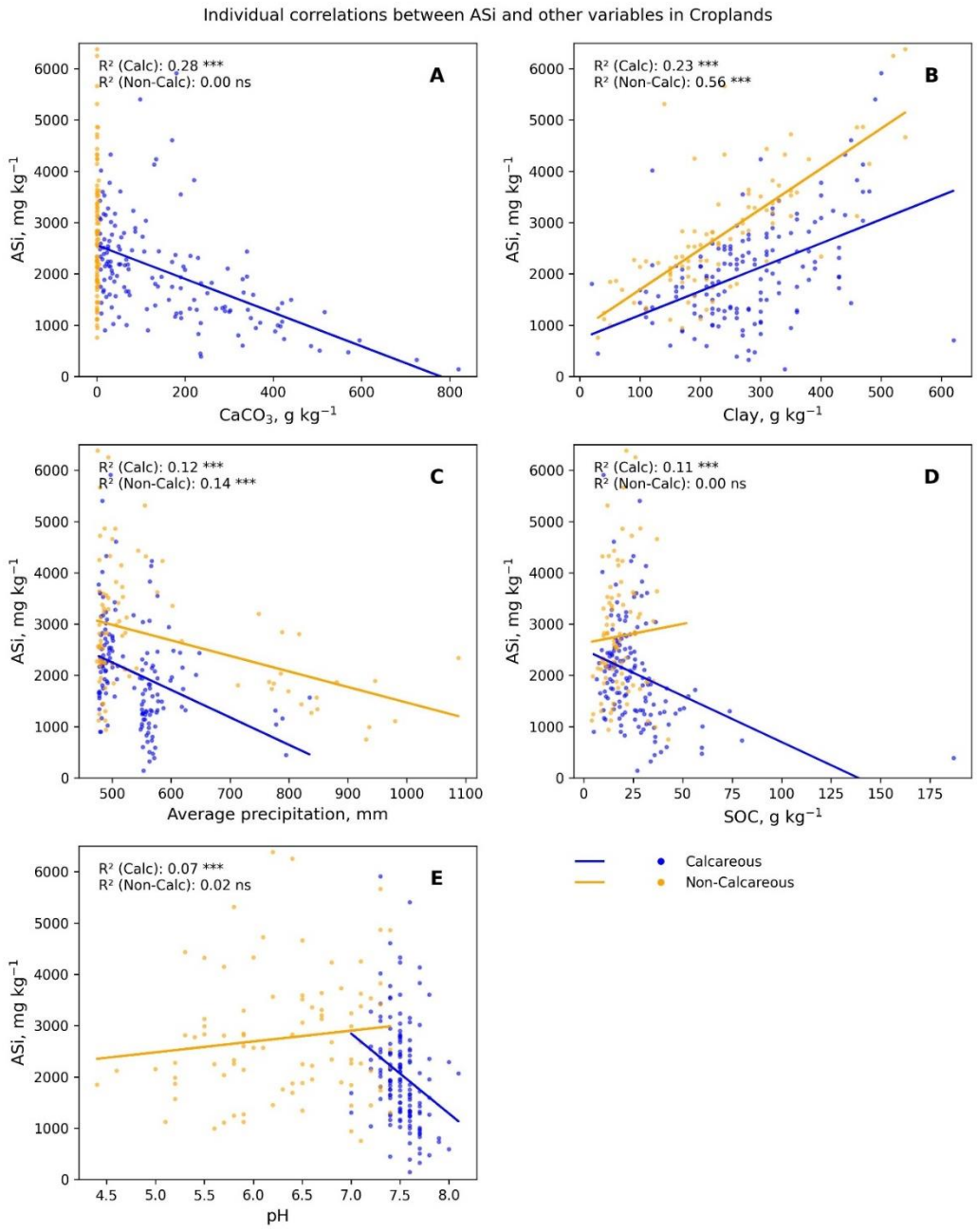


Fig. 3 Individual correlations between amorphous silica (ASi) and other variables in croplands for IS data. SOC: soil organic carbon. * indicates significant difference at $p \leq 0.05$, ** at $p \leq 0.01$, and *** at $p \leq 0.001$. For interpretation of the references to color in the Fig., please refer to the Web version of this article.

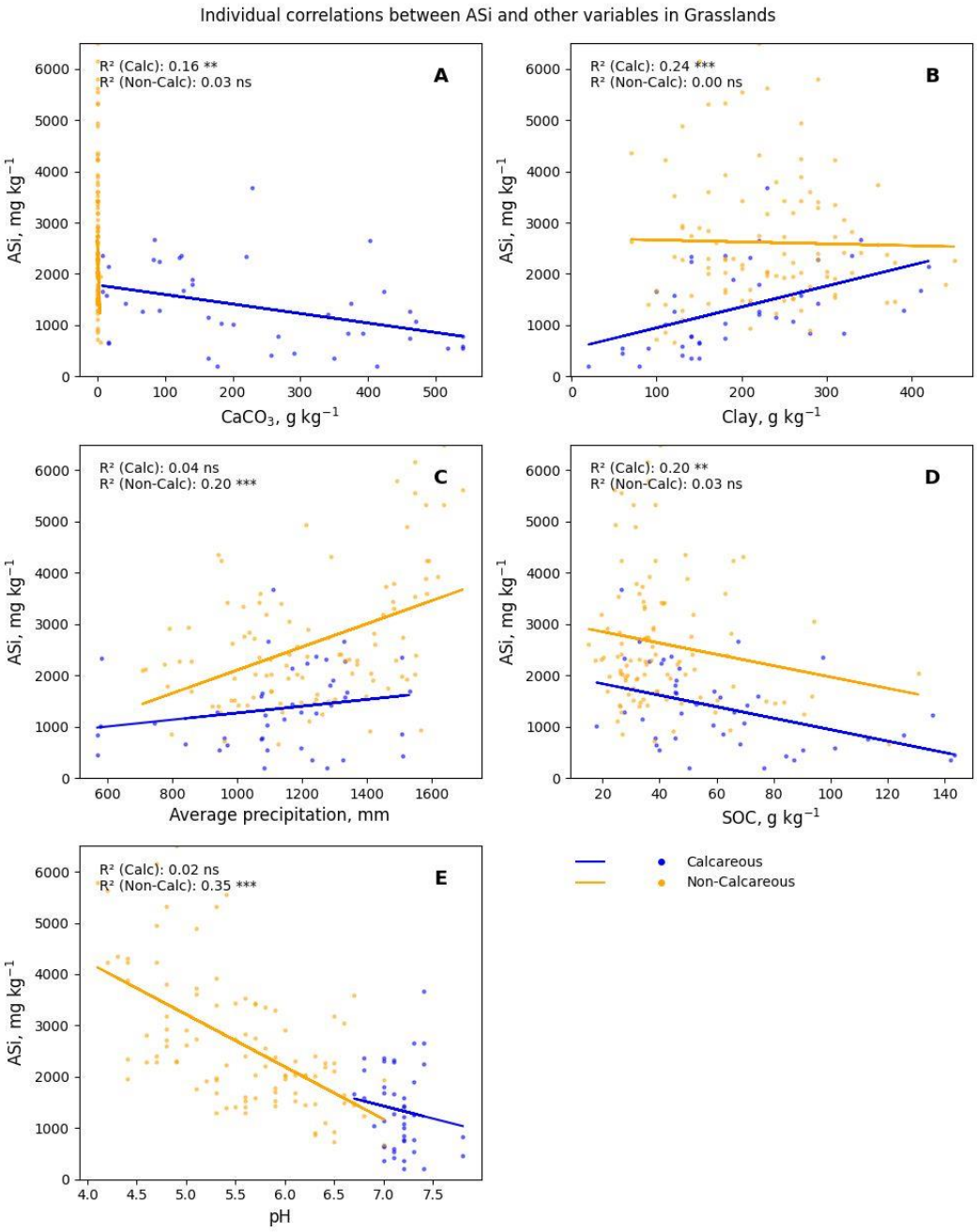


Fig. 4 Individual correlations between amorphous silica (ASi) and other variables in grasslands for IS data. SOC: soil organic carbon. * indicates significant difference at $p \leq 0.05$, ** at $p \leq 0.01$, and *** at $p \leq 0.001$. For interpretation of the references to color in the Fig., please refer to the Web version of this article.

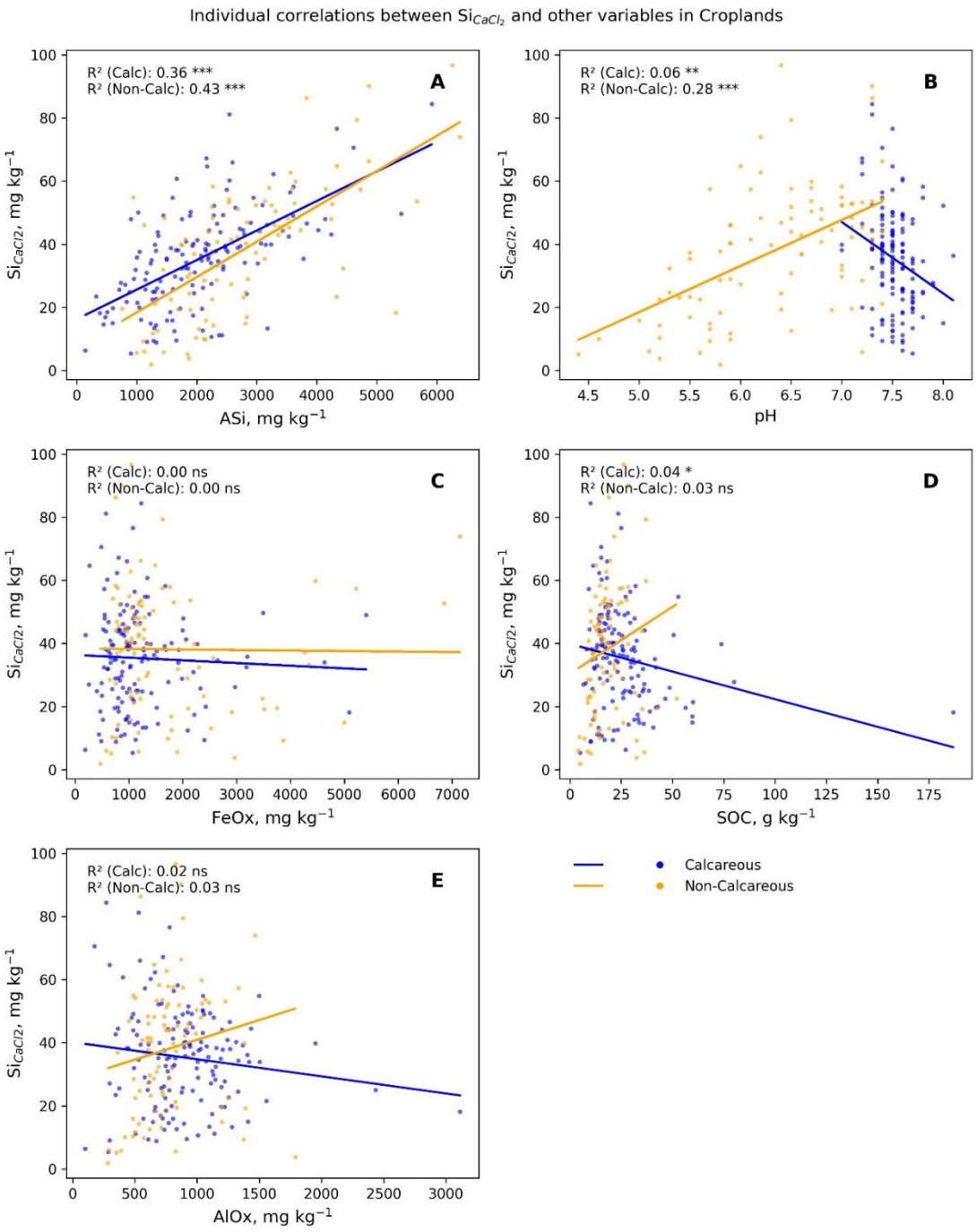


Fig. 5 Individual correlations between $CaCl_2$-extractable silicon ($Si_{CaCl2}$) and other variables in croplands for IS data. ASi: amorphous silica, AlOx and FeOx: acid ammonium oxalate extractable Al and Fe, respectively. SOC: soil organic carbon * indicates significant difference at $p \leq 0.05$, ** at $p \leq 0.01$, and *** at $p \leq 0.001$. For interpretation of the references to color in the Fig., please refer to the Web version of this article.

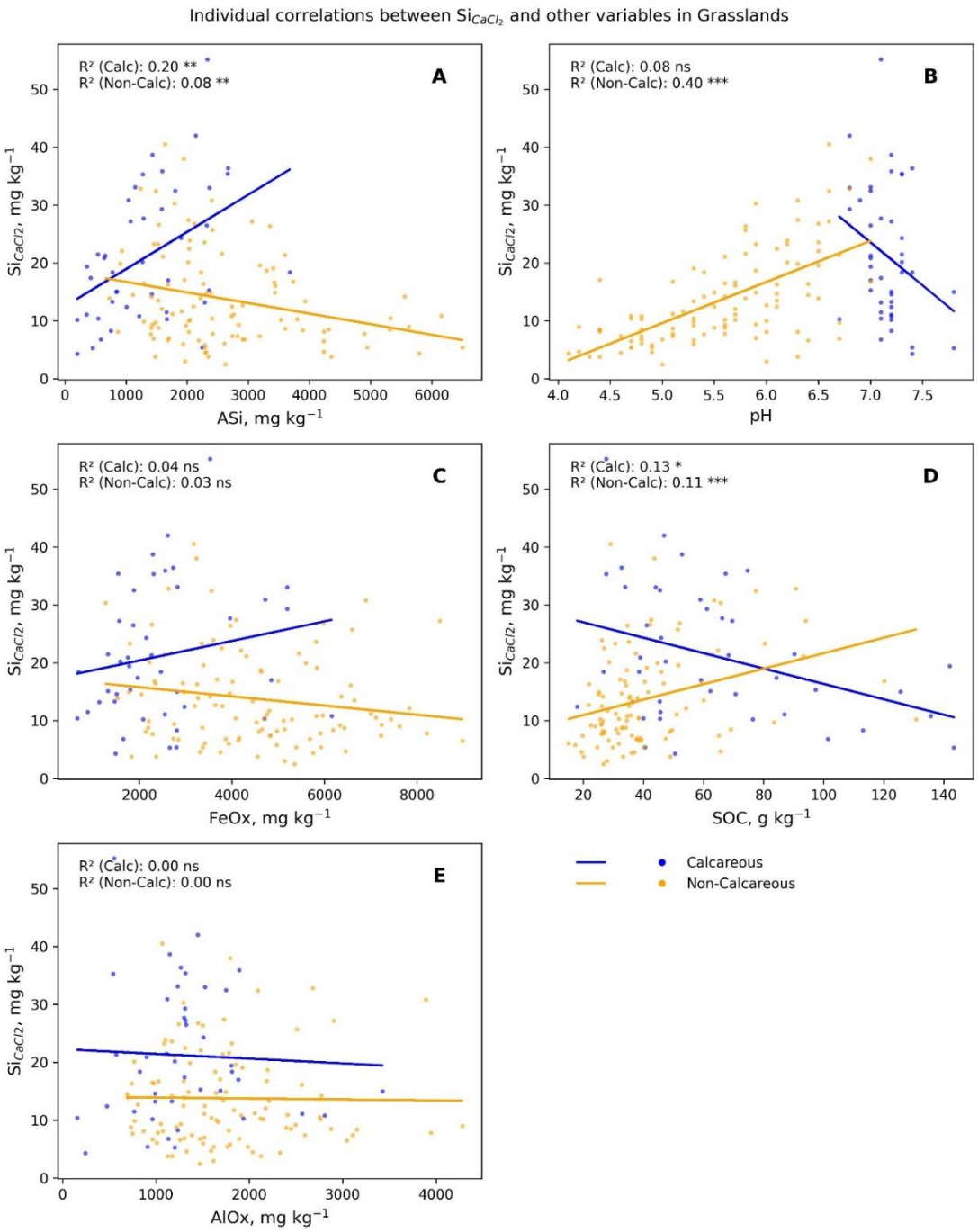


Fig. 6 Individual correlations between $CaCl_2$-extractable silicon ($Si_{CaCl2}$) and other variables in grasslands for IS data. ASi: amorphous silica, AlOx and FeOx: acid ammonium oxalate extractable Al and Fe, respectively. SOC: soil organic carbon * indicates significant difference at $p \leq 0.05$, ** at $p \leq 0.01$, and *** at $p \leq 0.001$. For interpretation of the references to color in the Fig., please refer to the Web version of this article.

## *Changes in soil si status between sampling campaigns*

The soil ASi concentrations did not significantly change between sampling campaigns (Fig. 7). The soil $Si_{CaCl2}$ concentrations increased significantly (Fig. 7) in non-calcareous grasslands (C) from a median of 11.1 to 15.1 mg kg$^{-1}$, and a mean ± StD of 13.8 ± 8.20 to 17.5 ± 8.20 mg kg$^{-1}$ and in calcareous croplands from a median of 35.3 to 37.3 mg kg$^{-1}$, and a mean ± StD of 35.2 ± 16.0 to 39.2 ± 15.8 mg kg$^{-1}$ (D). In calcareous grasslands (C) and non-calcareous croplands (D) no significant changes were observed.

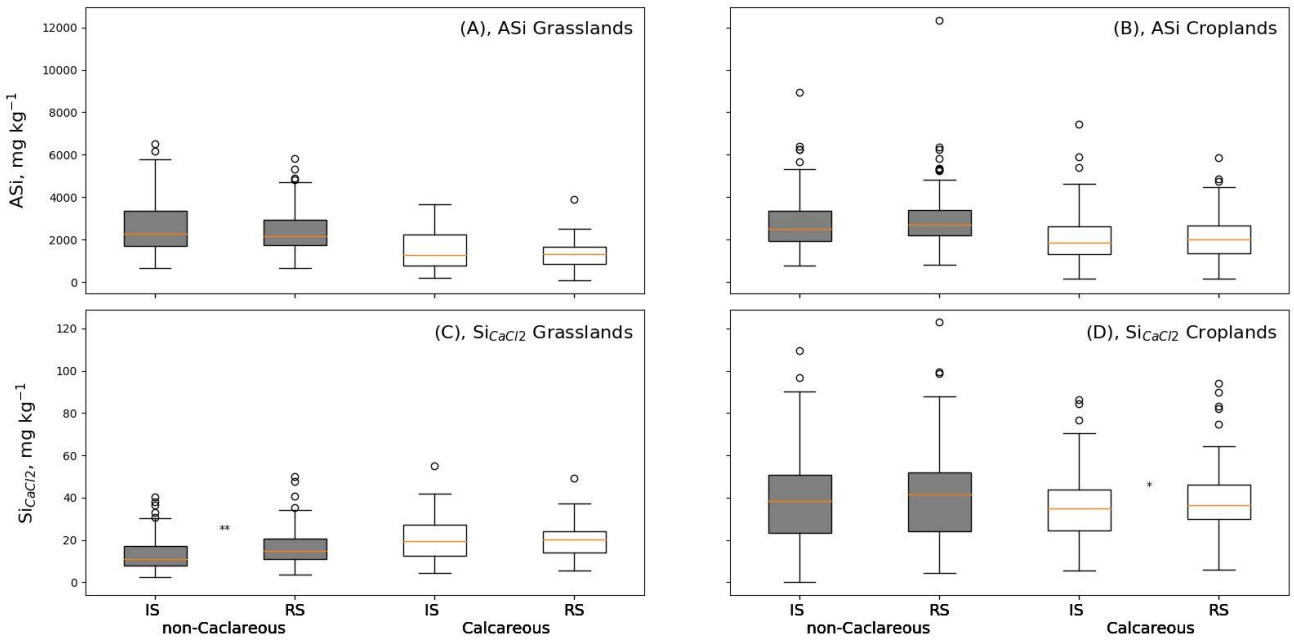


Fig. 7 Changes in soil ASi and $Si_{CaCl2}$ concentrations between sampling campaigns. A) ASi in grasslands, B) ASi in croplands, C) $Si_{CaCl2}$ in grasslands, D) $Si_{CaCl2}$ in croplands. * indicates significant difference at $p \leq 0.05$, ** at $p \leq 0.01$, and *** at $p \leq 0.001$. IS - Initial Sampling, RS - Resampling.

# DISCUSSION

## *Amorphous si*

Concentrations of ASi in the soils of this study (86-12300 mg kg$^{-1}$) are similar to those reported for other regions. Quigley *et al.* (2017) reported ASi concentrations ($Na_2CO_3$ extraction) ranging from 2000-14000 mg kg$^{-1}$ in savannas and plains of the Serengeti, Cornelis *et al.* (2010) ($Na_2CO_3$) 5500-14500 mg kg$^{-1}$ between 0 and 7.5 cm of brown forest soils (Alumnic, Cambisol) in France and Yang *et al.* (2019) reported mean ASi concentrations (NaOH) in the topsoil (0–10 cm) of grasslands in Inner Mongolia in China between $4350 \pm 200$ mg kg$^{-1}$ and $5840 \pm 620$ mg kg$^{-1}$ depending on the soil weathering stage. Vandevenne *et al.* (2015) reported ASi concentrations (NaOH) ranging between 4000-8000 mg kg$^{-1}$ in the top 50 cm of cropland soils in Belgium, Kaczorek *et al.* (2019) reported mean ASi concentrations (Tiron) ranging between 7510 ± 219 mg kg$^{-1}$ (0-3 cm) and 4400 ± 300 mg kg$^{-1}$ (3-23 cm) in grasslands and meadows, and 4710 ± 3 mg kg$^{-1}$ (0-30 cm) in croplands of Poland. It should be noted, however, that the extraction methods used in the mentioned studies differ partially from the one used in the current study ($Na_2CO_3$ *vs.* NaOH *vs.* Tiron). While the results can generally be similar (Stein *et al.*, 2024), the performance of these methods might vary under different soil conditions (Saccone *et al.*, 2007). We found only one study (Quigley *et al.*, 2017) which evaluated the impact of soil and environmental characteristics on soil ASi concentrations, however, in soils and under soil management practices (African savannas and plains) that are very different from the temperate, arable and grassland soils of this study. Using the structural equation model, those authors were able to explain 19% of the variability in soil ASi concentration by precipitation, soil pH, and sand content.

In the present study, ASi showed a negative association with soil $CaCO_3$ equivalent (Fig. 2A, B); these two parameters showed similar strength of correlation in croplands (Fig. 3A) and grasslands (Fig. 4A). Landré *et al.* (2020) observed a decrease in total Si correlated with an increase in soil $CaCO_3$ concentrations above 50 g kg$^{-1}$ and concluded that higher $CaCO_3$ concentrations 'dilute' the soil and result in smaller proportion of other soil components, including ASi. The likely most important effect of high $CaCO_3$ is an increase in soil pH, which results in the decrease of soil ASi concentration due to its solubilization and subsequent leaching, adsorption to clay particles, or enhanced plant uptake and removal by harvest (Haynes, 2019; Huang *et al.*, 2022; Miles *et al.*, 2014, de Tombeur *et al.*, 2020). In the study of de Tombeur *et al.* (2020), the authors observed $CaCO_3$ and soil ASi to be linked to differences in the soil development stage, as younger soils were higher in $CaCO_3$ and lower in ASi compared to soils in later stages of development in their 2 Ma chronosequence study in Western Australia. However, the soils investigated in this study are holocene soils that developed after the Würm glaciation with a maximum age of ~12000 years, so a strong relation of ASi content to differences in soil weathering is unlikely.

Soil ASi concentrations were positively associated with clay content (Fig. 2A, B), which was observed in both land use categories with the exception of non-calcareous grasslands (Fig. 3B, 4B). From the study of Georgiadis *et al.* (2015) it is known that part of the crystalline clay minerals contained in soil (*e.g.*, kaolinite, smectite) can be dissolved by alkaline solutions. Similar observations were made by Barão *et al.* (2014, 2015). A study of Keller *et al.* (2021) further supports this observation, showing that at least vermiculite is relatively soluble in NaOH solution. Such interference between soil clay content and extraction procedure means that part of the extracted Si may be wrongly attributed to ASi, while it originates in fact from a crystalline Si fraction. In addition to the potential dissolution of clay minerals, the clay particle size fraction may contain phytoliths ≤2 µm (Sommer *et al.*, 2006; Puppe *et al.*, 2017), which positively contribute to soil ASi concentrations (Fraysse *et al.*, 2006). However, we expect this contribution of clay-sized phytoliths to be rather small. Another potential effect of clay on ASi is that high clay content reduces the rate of $Si_{CaCl2}$ leaching, which allows $Si_{CaCl2}$ to precipitate upon drying, and thus favors the formation of minerogenic ASi (Drees *et al.*, 1989; Haynes, 2019).

Overall, the ASi concentrations were negatively associated with mean annual precipitation (Fig. 2A, B), but when plotted individually, the relation was negative in croplands (Fig. 3C), while there was no significant effect in calcareous grasslands and a positive correlation in non-calcareous grasslands (Fig. 4C). High levels of precipitation lead to more intense mineral weathering (Xie *et al.*, 2022), which may have several effects on soil Si. On the one hand, it may cause Si solubilization from minerals, which, if not leached, precipitates as ASi upon drying if the concentrations are sufficient, is adsorbed to soil particles, or taken up by plants (Drees *et al.*, 1989; Haynes, 2019), but the effect of increased mineral weathering is expected to be rather small. On the other hand, high precipitation rates favor also the dissolution of ASi (Blecker *et al.*, 2006; Drees *et al.*, 1989; Quigley *et al.*, 2017), especially at the favorable pH values (median 6.5) observed in the cropland soils of our study region. In our dataset, an increase in the precipitation rate is associated with an increase in altitude, a decrease in soil depth and an increase in the slope which may not only inhibit ASi precipitation through increased leaching of dissolved Si (Van Tol *et al.*, 2013; Dixon *et al.*, 2016; Evans and Cox, 1999), but also contribute to ASi particles being washed down and eventually out of the soil profile (Clymans *et al.*, 2015; Smis *et al.*, 2011). Therefore, we assume that the observed decrease of ASi with increasing precipitation rates in cropland soils is primarily explained by ASi solubilization and subsequent leaching of Si. In contrast, the lower pH of non-calcareous grassland soils (median pH 5.6) may explain the observed increase of ASi with increasing precipitation, as at low pH the solubility of primary minerals is enhanced whereas ASi solubility is low, thus supporting ASi accumulation following primary mineral weathering. Our interpretation of the effects of precipitation on ASi are supported by reported dissolution rates of primary mineral, clays and phytoliths (Fraysse *et al.*, 2009).

Overall, ASi was negatively associated with SOC (Fig. 2A, B). Individual negative correlations were observed only in calcareous soils (Fig. 3D, 4D). This observation contrasts the results of Alfredsson *et al.* (2016) and Clymans *et al.* (2013), who found a positive association, which these authors interpreted as simultaneous increases in soil SOC and ASi linked to biomass inputs. Both studies, however, were performed in rather specific conditions (arctic soils with no or almost no agricultural activity and a field-scale experiment, comparing two different management practices) and thus cannot be directly compared to ours. In our study, we investigated ASi across various soil groups, including hydromorphic soils (Gleysols, Histosols). As shown in Table II, the Gleysols have distinctly lower ASi than soils formed under terrestrial conditions. Hydromorphic conditions in Gleysols favor the accumulation of organic matter due to limited oxygen supply for microbial mineralization. Moreover, they are typically characterized by inhibited weathering of primary minerals due to limited leaching and oxygen availability. Inhibited weathering may explain lower ASi in these soils which, as indicated before, are characterized by high SOC. In Histosols, by definition, exhibiting SOC concentrations > 200 g $kg^{-1}$, the limited amount of mineral fraction is expected to further reduce the formation of ASi. All together, the observed negative relation between SOC and ASi in our study can be related to the coincidence of large SOC concentrations, inhibited formation of ASi, and dilution of the mineral phase by organic matter.

Soil pH was negatively associated with ASi (Fig. 2A, B), which was expected as the solubility of ASi strongly increases with increasing pH (Haynes, 2019; Huang *et al.*, 2022; Miles *et al.*, 2014). A negative correlation between ASi and pH was observed by both Quigley *et al.* (2017) and Caubet *et al.* (2020). Interestingly, when plotted individually, a weak negative correlation of pH and ASi concentration was observed in calcareous croplands, but not in non-calcareous croplands (Fig. 3E), while a clear negative correlation was observed in non-calcareous grasslands, but no correlation in calcareous grasslands (Fig. 4E). The weak and lacking correlations with pH in calcareous soils are likely related to their strong pH buffering in their narrow pH range. Under these conditions, other factors (mainly $CaCO_3$ and clay content) are much more important controls of ASi than pH. In calcareous grasslands, the increase in primary mineral weathering with decreasing pH, associated with increasing ASi solubility at high pH values as described above, likely explains the distinctly negative correlation of pH and ASi concentration.

*$Cacl_2$-extractable silicon fraction*

The concentrations of $Si_{CaCl2}$ found in this study (3.7 to 123 mg $kg^{-1}$ with a median of 30 mg $kg^{-1}$) are similar to those reported by Caubet *et al.* (2020) for France (2.3 to 134 mg $kg^{-1}$; median 17 mg $kg^{-1}$). The difference in the median value is likely due to the wider sampling geography and thus parent material in their study. Our model performance was close to that of Caubet *et al.* (2020), who used the same model. While only some of the explanatory variables were used in both studies, those having the highest impact on $Si_{CaCl2}$ concentrations were generally the same: pH and clay content. In our model for $Si_{CaCl2}$, clay was excluded due to its strong correlation with ASi concentrations, which could have introduced autocorrelation. However, an indirect, positive impact of soil clay content on $Si_{CaCl2}$ can be expected, as clay content is positively correlated with soil ASi concentration. This correlation is due to clays providing sorption sites for soluble Si species, which has the potential of reducing $Si_{CaCl2}$ leaching (Caubet *et al.*, 2020), and as clay is a source of plant-available Si (Keller *et al.*, 2021). Indeed, when plotted individually (data not shown), positive correlations between $Si_{CaCl2}$ and clay were evident in all land use categories with the exception of calcareous grasslands.

The results of $Si_{CaCl2}$ modeling using the structural equation model (Quigley *et al.* (2017), were similar to the results of this study. In their study, 74% of the variability in $Si_{CaCl2}$ among 63 soils of the Serengeti were explained by precipitation, soil pH and sand content. The role of sand in their study was attributed to its impact on plant community composition and also to the fact that high sand content promotes leaching of $Si_{CaCl2}$, as well as the translocation of small phytoliths to the groundwater, thus resulting in limited recycling. In comparison, our model explained 54% of the variability in $Si_{CaCl2}$ for our dataset, using similar explanatory variables.

Amorphous Si and pH were both positively associated with soil $Si_{CaCl2}$ in our work. Individual plots show positive correlation between ASi and $Si_{CaCl2}$ in cropland soils (Fig. 5A) and calcareous grasslands, but a negative correlation in non-calcareous grasslands (Fig. 6A). Moreover, $Si_{CaCl2}$ is positively correlated with pH in non-calcareous croplands and grasslands, while it is only weakly, and only partly significantly correlated with pH in calcareous soils, again mostly because the pH range in calcareous soils is very small (Fig. 5B and 6B). The solubilization of ASi is a main source of soil $Si_{CaCl2}$, as its solubility exceeds that of other Si-containing soil minerals by $10^2$ - $10^4$ times (Fraysse *et al.*, 2006), and is highly dependent on soil pH (Haynes, 2019; Huang *et al.*, 2022; Miles *et al.*, 2014). The importance of ASi in determining $Si_{CaCl2}$ increases with the progress of weathering (Cornelis and Delvaux, 2016), and at the late stages of soil development, biogenic ASi, together with Si previously adsorbed to FeOx, as well as the dissolution of kaolinite (de Tombeur *et al.*, 2020), are believed to be important sources of $Si_{CaCl2}$. The process of ASi solubilization can be roughly described as following: water dissolves $SiO_2$ by breaking siloxane bonds (Si–O–Si), which results in the formation of silanol groups (Si–OH). At pH values above pH 4, deprotonation of existing silanol groups occurs, resulting in formation of siloxide ions ($Si\text{-}O^-$), which further destabilize the structure and contribute to breaking of siloxane bonds (Dove *et al.*, 2008; Fraysse *et al.*, 2006). The breaking of these bonds allows for further hydrolysis of siloxane, resulting in the formation of new silanol groups. These newly formed silanol groups can then undergo further hydrolysis or deprotonation, ultimately leading to the release of $Si_{CaCl2}$. In general, our findings are well aligned with those of studies in France (Caubet *et al.*, 2020), Panama (Schaller *et al.*, 2018), India (Meunier *et al.*, 2018), South Africa (Miles *et al.*, 2014), and Poland (Struyf *et al.*, 2009), all of which reported a positive correlation between soil pH and/or ASi concentrations with $Si_{CaCl2}$ concentrations.

The RF model indicates a negative association of FeOx content with $Si_{CaCl2}$ concentrations (Fig. 2) in our soil dataset, however with a much smaller overall impact than ASi and pH. The individual correlations between FeOx and $Si_{CaCl2}$ were not significant. (Fig. 5C, 6C). This observation is opposite to those of de Tombeur *et al.* (2020) and Caubet *et al.* (2020), who found a positive correlation between soil $Si_{CaCl2}$ and FeOx content, of Cornu *et al.* (2022), who observed no such correlation, and similar to those of McKeague and Cline (1963), who found a weak negative correlation. $Si_{CaCl2}$ interacts with the surfaces of metal oxides by forming inner-sphere complexes (Hiemstra *et al.*, 2007) which results in the removal of $Si_{CaCl2}$ from the soil solution. The process is pH-dependent (Dietzel, 2002; Haynes, 2014; Hiemstra *et al.*, 2007), with peak adsorption at pH 9.8 (Dietzel, 2002).

In this study, the effect of AlOx content on $Si_{CaCl2}$ was similar to that of FeOx but lower in magnitude (Fig. 2, 5E, 6E). $Si_{CaCl2}$ adsorbs to surfaces of AlOx (Goldberg and Glaubig, 1988) leading to the removal of $Si_{CaCl2}$ from solution starting at pH 4 with an increase in sorption intensity up to pH 9. The negative impact of AlOx on soil $Si_{CaCl2}$ was also demonstrated by Jones and Handreck (1963). Thus, high FeOx and AlOx concentrations lead to the adsorption of orthosilicate to the oxides surfaces and so to a decrease in $Si_{CaCl2}$ concentrations in soil solution at typical soil pH ranges, while at low soil pH they release $Si_{CaCl2}$, thus serving as a source (de Tombeur *et al.*, 2020).

Overall, $Si_{CaCl2}$ concentrations were negatively correlated with SOC (Fig. 2). Plotted individually, $Si_{CaCl2}$ was positively correlated with SOC in non-calcareous grasslands, and negatively in calcareous grasslands (Fig. 6D). Our observations here are differ from observations of Yang *et al.* (2021), who reported a positive correlation and explained it by SOC being a proxy for phytoliths, and from observations of Caubet *et al.* (2020), who also reported

positive correlations. However, the effect of SOC on $Si_{CaCl2}$ was, similar to the observations of Caubet at al. (2020), rather weak and inconsistent in the present study. Overall, the correlation between $Si_{CaCl2}$ and SOC is difficult to explain with the available data and more detailed investigation is required to elucidate this aspect.

### *Changes in soil si status between sampling campaigns*

#### Changes in ASi concentrations

In our study, ASi concentrations did not change significantly (Fig. 7A) between the sampling campaigns. The only available study comparing ASi concentrations in temperate zone soils over time is that of Guntzer *et al.* (2012). They evaluated Si dynamics in the Broadbalk continuous winter wheat experiment in Rothamsted, and showed a decrease in ASi concentrations in the topsoil (25 cm) after about 100 years of wheat cultivation, which the authors associated with the export of Si-rich wheat straw from the field. In addition, Keller *et al.* (2012) suggested that changes in soil pH also played a role in the observed decrease of ASi concentrations in the study of Guntzer *et al.* (2012). Clymans *et al.* (2011) suggested that soil cultivation leads to a decrease in soil ASi. According to their estimations, the soil ASi pool in the temperate zone decreased by approximately 10% since the onset of agricultural development (3000 BCE), mostly due to the changes in land use from forests to grasslands or croplands within the last 250 years. Similarly, Carey and Fulweiler (2016) highlighted that the global production of the ten major crops nearly tripled in the past 50 years, which significantly increased Si uptake, potentially reducing soil ASi in croplands. Given the data of Clymans *et al.* (2011), it seems very unlikely that significant changes in the relatively large and, within this time period, stable ASi fraction could have occurred within 20-30 years of constant land use in temperate zone soils in the present study.

#### Changes in $Si_{CaCl2}$ concentrations

A significant increase in $Si_{CaCl2}$ concentrations was observed in calcareous croplands (median: 35.3 to 37.3 mg $kg^{-1}$, 5.7%) and in non-calcareous grasslands (median from 11.1 to 15.1 mg $kg^{-1}$, 32.4%) (Fig. 7C, D) between the initial and the second soil sampling campaign. In this period, major changes in the agronomic management of these soils occurred, which affected *e.g.* the SOC content of the soils in this area (Wenzel *et al.*, 2022), and may also contribute to changes in $Si_{CaCl2}$. In 1993, during the initial soil sampling campaign, open biomass (straw) incineration was prohibited in Austria (BGBl. Nr. 405/1993), which was a common practice at the time, especially in eastern Austria, where the low soil water availability was often insufficient for microbial biomass mineralization. In 1995, agri-environmental measures were implemented through the ÖPUL program, aiming at promoting sustainable agricultural practices. An important aim of ÖPUL is to increase SOC stocks in soils, with cover cropping being one of the major measures to reach this aim. Both these changes may have increased $Si_{CaCl2}$ in calcareous croplands: Biomass burning was shown to decrease the solubility of phytoliths (Li *et al.* 2024), so the cessation of straw burning likely increased phytolith solubility and thus $Si_{CaCl2}$. In addition, growing cover crops after the main crop, and their incorporation into the soil before the start of the following growing season, may have increased the production and introduction of phytoliths to the soil.

The reasons for the observed increase in $Si_{CaCl2}$ in non-calcareous grasslands are less obvious, as changes in grassland management include both intensification and extensification (Wenzel *et al.*, 2022). The same authors, using a largely overlapping dataset, observed clear increases of the SOC concentrations beneath grassland in the same monitoring period, probably due to increased biomass production on these sites, which in turn could be linked to increased phytolith input to these soils. Moreover, Wenzel (unpublished data) observed a decrease of the pH in the non-calcareous grassland soils in the study area during the same period from on average ~ 5.50 to ~ 5.25, likely contributing to increased $Si_{CaCl2}$ through enhanced mineral weathering.

### *Impact of $si_{cacl2}$ concentrations on plant production*

Grasses, including wheat (Mayland *et al.*, 1991), rice (Ma *et al.*, 2006), and sugarcane (Savant *et al.*, 1999), concentrate 1-3%, and sometimes up to even 10% of Si in their shoots. Threshold levels of $Si_{CaCl2}$ concentration in soil have been proposed to be 43 mg $kg^{-1}$ for rice (Narayanaswamy and Prakash, 2009) and 20 mg $kg^{-1}$ for sugar cane (Haysom and Chapman, 1975), respectively. Although no soil $Si_{CaCl2}$ threshold values have been proposed for other (gramineous) crops like wheat, some authors (*e.g.*, Caubet *et al.*, 2020) argued that 20 mg $kg^{-1}$ and 43 mg $kg^{-1}$ could be adopted, as the average wheat shoot Si concentration is between those of sugarcane and rice (Hodson *et al.*, 2005). It is important to note that for a beneficial (non-essential) element for plants like Si, there is, strictly speaking, no 'threshold' below which a crop is insufficiently supplied. However, for practical purposes it is necessary to define a

value below which beneficial responses of a crop to the addition (fertilization) of the element can be reasonably expected. Therefore, we use the term 'threshold' here in this broad and general sense. Accordingly, 5.6% and 66.7% and 18.2% and 52.7% of calcareous and non-calcareous croplands in this study are below the lower and upper threshold value, respectively, (Fig. 8). Note that sugarcane and rice are both strong Si-accumulating crops grown on very different soils and climates, thus comparisons with cereals of the temperate zones require caution. For example, in a study of Monoshyn *et al.* (2024), a linear increase in wheat shoots Si concentrations was observed when $Si_{CaCl2}$ increased from 5 to 20 mg $kg^{-1}$, but no correlation between shoots Si and $Si_{CaCl2}$ was seen in the 30 to 70 mg $kg^{-1}$ range. Although these authors used only two soil types and one variety of wheat, these data indicate that an increase in $Si_{CaCl2}$ above 30 mg $kg^{-1}$ may not result in an increased Si uptake in wheat. Si fertilization has been demonstrated to have a positive impact on wheat productivity under stress conditions (Walsh *et al.*, 2018), therefore it might increase yield stability on cropland sites, however, threshold values for Si fertilization need to be established using a sufficiently large number of region-specific field trials.

As for grasslands, we are not familiar with any attempts to establish soil-Si thresholds, however, Si fertilization has been shown to have a positive impact on the productivity of grasslands (Borawska-Jarmułowicz *et al.*, 2022) as well. Given that many grassland species accumulate similar shoot Si concentrations as cereals (*e.g.*, ryegrass up to 4%; Nanayakkara *et al.*, 2008), we compare the observed $Si_{CaCl2}$ values with the thresholds for rice and sugar cane, well knowing that the establishment of actual thresholds can only be based on a set of field fertilization experiments. However, this comparison shows that among the sampled grasslands, 49% and 98% and 71.1% and 97.9% of calcareous and non-calcareous ones, respectively, are below the lower and higher thresholds (Fig. 8). Accounting for the scarce number of studies attempting to establish whether and at which levels Si fertilization has a positive effect in different soil type and/or production scenarios, detailed and extensive field studies are needed.

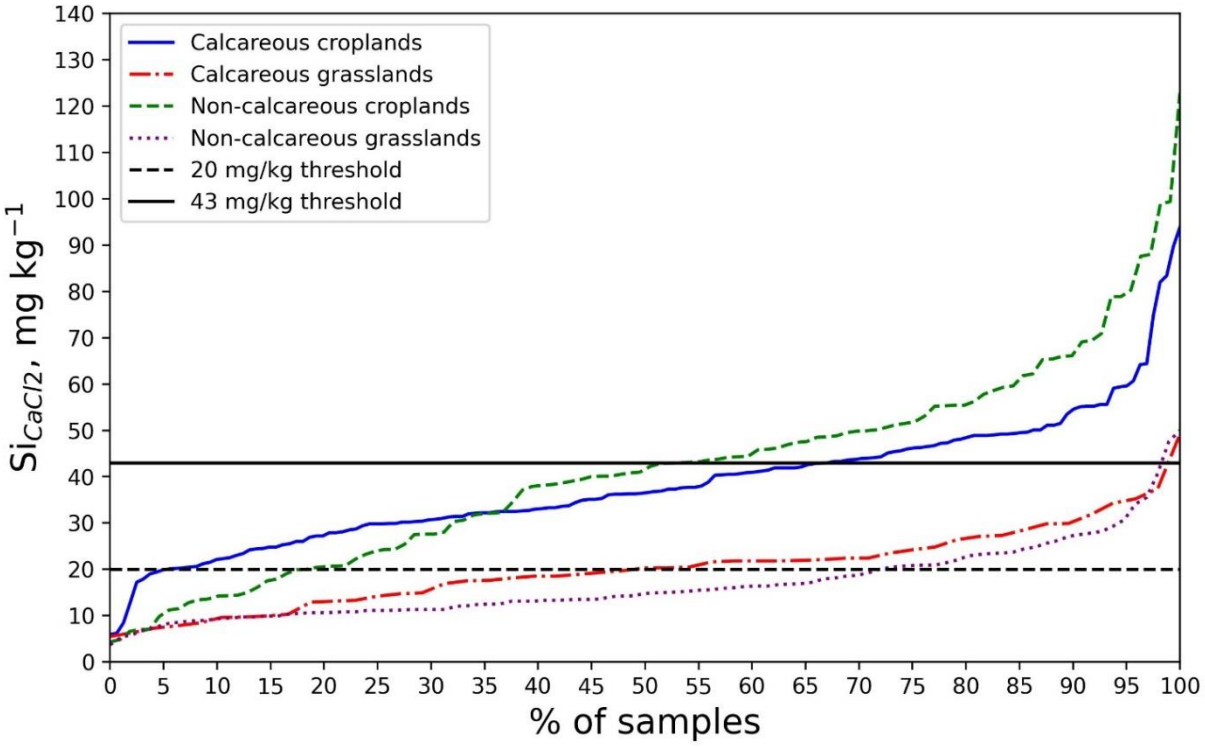


Fig. 8 $Si_{CaCl2}$ concentrations in calcareous croplands, calcareous grasslands, non-calcareous croplands, and non-calcareous grasslands. The dashed horizontal line represents the proposed 20 mg $kg^{-1}$ $Si_{CaCl2}$ threshold for sugar cane (Haysom and Chapman, 1975), the solid horizontal line represents the proposed 43 mg $kg^{-1}$ threshold for rice (Narayanaswamy and Prakash, 2009). The sample numbers are shown as percentages for each group, as the group sizes are not equal. For interpretation of the references to color in the Fig., please refer to the Web version of this article.

## *Limitations of the study*

This study was carefully designed and conducted but has some inherent limitations that are caused by the sampling conditions as well as the experimental and statistical methods used. There is some spatial variability associated with the exact re-location of the initial sampling site, however, as described above, we reduced this issue as much as possible. The selectivity of all soil extraction methods, including the NaOH ASi extraction used here (Stein *et al.*,

2024), are limited to some extent by the dissolution of Si from other minerals such as clays, however, many soil extraction methods suffer from the difficult task of extracting chemically distinct species from a vast mixture of substances. As is the usual way of handling this problem, we interpreted our data carefully and acknowledge that the soil ASi fraction encompasses small contributions from clay mineral dissolution. Moreover, the cluster-nature of the sampling campaign, as well as unequal numbers of sampled sites for each category could result in model bias towards bigger groups. However, the consistent results of cross-validation among folds indicate a good degree of generalization despite this imbalance.

# CONCLUSIONS

The concentrations of amorphous silica and $CaCl_2$-extractable silicon observed in this study are well within the ranges reported by other studies for similar soil climatic conditions. The median concentrations of amorphous silica decreased in the order *non-calcareous croplands* > *non-calcareous grasslands* > *calcareous croplands* > *calcareous grasslands*, while $CaCl_2$-extractable silicon decreased in the order *non-calcareous croplands* > *calcareous croplands* > *calcareous grasslands* > *non-calcareous grasslands*. The major factors explaining soil ASi concentrations were soil $CaCO_3$ and clay content, while ASi content and soil pH determined $Si_{CaCl2}$ concentrations strongly. Soil ASi status did not change within the 20-30-year period between initial and resampling in this study, however, in calcareous croplands and non-calcareous grasslands, increased $Si_{CaCl2}$ concentrations were observed that were most likely caused by soil management changes (*i.e.* intensification of land use, introduction of cover cropping, changes in litter management policy). A large share of the soils in the study region are falling below thresholds for $CaCl_2$-extractable Si which have been proposed for sugarcane and rice in tropical and subtropical conditions. Our findings may be an indication of limited Si availability for cereal and maybe legume crops in arable farming, but also for grass species in grasslands. Given the increasing drought stress in the study area, Si supply to crop species is a promising management option to reduce stress-induced yield losses. Therefore, further studies on the feasibility of Si fertilization in this cropping area are required. Sites identified as having $CaCl_2$-extractable Si concentrations below 20 mg/kg are especially well-suited for future Si fertilization experiments.

# DECLARATION OF COMPETING INTEREST

The authors declare that they have no known competing financial interests or personal relationships that could have appeared to influence the work reported in this paper.

# ACKNOWLEDGMENT

The authors are thankful to Mariia Morozova for her help with the SHAP plots preparation, to Ekaterina Shaymullina - for initial proofreading, to Elena Cocuzza, Johanna Reiter and Anna Schiefer for conducting the soil re-sampling campaign and the ASi and $Si_{CaCl2}$ analyses, and to Lower Austria province and geomap.at for providing high-quality map service and competent consultation.

# FUNDING

This work was supported by the Lower Austrian Landscape Fund, project number ABB-LEBO-498/0002. It also received funding from the Austrian Science Fund (FWF) and the province of Lower Austria, project number P31808-BBL.

# SUPPLEMENTARY MATERIAL

Supplementary material for this article can be found in the online version.

# CONTRIBUTION OF AUTHORS

Jakob SANTNER and Walter W. WENZEL contribute equally to this work.

## DECLARATION OF GENERATIVE AI AND AI-ASSISTED TECHNOLOGIES IN THE WRITING PROCESS

During the preparation of this work, the authors used ChatGPT 4/3.5 for occasional spelling, grammar and formulation checking, as well as for the primary debugging of code. After using this service, the authors reviewed and edited the content as needed and take full responsibility for the content of the publication.

## REFERENCES


Alfredsson, H., Clymans, W., Hugelius, G., Kuhry, P., Conley, D.J., 2016. Estimated storage of amorphous silica in soils of the circum-Arctic tundra region. *Glob. Biogeochem. Cycles.* **30**: 479–500.

Barão, L., Clymans, W., Vandevenne, F., Meire, P., Conley, D.J., Struyf, E., 2014. Pedogenic and biogenic alkaline-extracted silicon distributions along a temperate land-use gradient. *Eur. J. Soil Sci.* **65**: 693–705.

Barão, L., Vandevenne, F., Clymans, W., Frings, P., Ragueneau, O., Meire, P., Conley, D.J., Struyf, E., 2015. Alkaline-extractable silicon from land to ocean: A challenge for biogenic silicon determination. *Limnol. Oceanogr. Methods*.**13**: 329–344.

Bénard, C., Da Veiga, S., Scornet, E., 2022. Mean decrease accuracy for random forests: inconsistency, and a practical solution *via* the Sobol-MDA. *Biometrika*.**109**:881–900.

BFW, 2023. eBOD2 [WWW Document]. URL https://bodenkarte.at/

BGBl. Nr. 405/1993, 1993. Federal Act on a Ban on the Burning of Biogenic Materials Outside Installations. BGBl (In German). Nr. 405/1993.

Bindi, M., Olesen, J.E., 2011. The responses of agriculture in Europe to climate change. *Reg. Environ. Change* .**11**: 151–158.

Birchall, J.D., 1995. The essentiality of silicon in biology. *Chem. Soc. Rev.* **24**: 351.

Blecker, S.W., McCulley, R.L., Chadwick, O.A., Kelly, E.F., 2006. Biologic cycling of silica across a grassland bioclimosequence. *Glob. Biogeochem. Cycles*.**20**.

Bokor, B., Santos, C.S., Kostoláni, D., Machado, J., da Silva, M.N., Carvalho, S.M.P., Vaculík, M., Vasconcelos, M.W., 2021. Mitigation of climate change and environmental hazards in plants: Potential role of the beneficial metalloid silicon. *J. Hazard. Mater.* **416**: 126193.

Borawska-Jarmułowicz, B., Mastalerczuk, G., Janicka, M., Wróbel, B., 2022. Effect of Silicon-Containing Fertilizers on the Nutritional Value of Grass–Legume Mixtures on Temporary Grasslands. *Agriculture* **12**: 145.

Breiman, L., 2001. Random Forests. *Mach. Learn.* **45**: 5–32.

Carey, J.C., Fulweiler, R.W., 2016. Human appropriation of biogenic silicon – the increasing role of agriculture. *Funct. Ecol.* **30**: 1331–1339.

Casey, W.H., Kinrade, S.D., Knight, C.T.G., Rains, D.W., Epstein, E., 2004. Aqueous silicate complexes in wheat, Triticum aestivum L. *Plant Cell Environ.* **27**: 51–54.

Caubet, M., Cornu, S., Saby, N.P.A., Meunier, J.-D., 2020. Agriculture increases the bioavailability of silicon, a beneficial element for crop, in temperate soils. *Sci. Rep.* **10**: 19999.

Chen, C., Lewin, J., 1969. Silicon as a nutrient element for Equisetum arvense. *Can. J. Bot.* **47**: 125–131.

Clymans, W., Struyf, E., Govers, G., Vandevenne, F., Conley, D.J., 2011. Anthropogenic impact on amorphous silica pools in temperate soils. *Biogeosciences* **8**: 2281–2293.

Clymans, W., Struyf, E., Van den Putte, A., Langhans, C., Wang, Z., Govers, G., 2015. Amorphous silica mobilization by inter-rill erosion: insights from rainfall experiments. *Earth Surf. Process. Landf.* **40**: 1171–1181.

Clymans, W., Verbeeck, T., Tielens, S., Struyf, E., Vandevenne, F., Govers, G., 2013. Amorphous Silica Preservation in an Anthropogenic Soil: An Explorative Study of “Plaggen” Soils, in: Progress in Silicones and Silicone-Modified Materials, ACS Symposium Series. American Chemical Society, pp. 3–14.

Conley, D.J., 2002. Terrestrial ecosystems and the global biogeochemical silica cycle. *Glob. Biogeochem. Cycles* **16**, 68-1-68–8.

Cornelis, J.-T., Delvaux, B., 2016. Soil processes drive the biological silicon feedback loop. *Funct. Ecol.* **30**.

Cornelis, J.-T., Titeux, H., Ranger, J., Delvaux, B., 2010. Impact of tree species on the distribution of amorphous silica in an acid brown soil. Presented at the 19th World Congress of Soil Science, Soil Solutions for a Changing World, Brisbane, Australia.

Cornu, S., Meunier, J.-D., Ratie, C., Ouedraogo, F., Lucas, Y., Merdy, P., Barboni, D., Delvigne, C., Borschneck, D., Grauby, O., Keller, C., 2022. Allophanes, a significant soil pool of silicon for plants. *Geoderma* **412**: 115722.

Darmawan, Kyuma, K., Saleh, A., Subagjo, H., Masunaga, T., Wakatsuki, T., 2006. Effect of long-term intensive rice cultivation on the available silica content of sawah soils: Java Island, Indonesia. *Soil Sci. Plant Nutr.* **52**: 745–753.

de Tombeur, Felix, Turner, B.L., Laliberté, E., Lambers, H., Cornelis, J.-T., 2020. Silicon Dynamics During 2 Million Years of Soil Development in a Coastal Dune Chronosequence Under a Mediterranean Climate. *Ecosystems* **2**: 1614–1630.

Dietzel, M., 2002. Interaction of polysilicic and monosilicic acid with mineral surfaces, in: Stober, I., Bucher, K. (Eds.), Water-Rock Interaction. Springer Netherlands, Dordrecht, pp. 207–235.

Dixon, J.L., Chadwick, O.A., Vitousek, P.M., 2016. Climate-driven thresholds for chemical weathering in postglacial soils of New Zealand. *J. Geophys. Res. Earth Surf.* **121**: 1619–1634.

Dove, P.M., Han, N., Wallace, A.F., De Yoreo, J.J., 2008. Kinetics of amorphous silica dissolution and the paradox of the silica polymorphs. *Proc. Natl. Acad. Sci.* **105**: 9903–9908.

Drees, R.L., Wilding, L.P., Smeck, N.E., Senkayi, A.L., 1989. Silica in Soils: Quartz and Disordered Silica Polymorphs, in: Minerals in Soil Environments. John Wiley & Sons, Ltd, pp. 913–974.

Evans, I.S., Cox, N.J., 1999. Relations between land surface properties: Altitude, slope and curvature, in: Hergarten, S., Neugebauer, H.J. (Eds.), Process Modelling and Landform Evolution, Lecture Notes in Earth Sciences. Springer, Berlin, Heidelberg, pp. 13–45.

Fraysse, F., Pokrovsky, O.S., Schott, J., Meunier, J.-D., 2006. Surface properties, solubility and dissolution kinetics of bamboo phytoliths. *Geochim. Cosmochim. Acta* **70**, 1939–1951.

Fraysse, F., Pokrovsky, O.S., Schott, J., Meunier, J.-D., 2009. Surface chemistry and reactivity of plant phytoliths in aqueous solutions. *Chem. Geol.* **258**: 197–206.

Georgiadis, A., Sauer, D., Breuer, J., Herrmann, L., Rennert, T., Stahr, K., 2015. Optimising the extraction of amorphous silica by NaOH from soils of temperate-humid climate. *Soil Res.* **53**: 392.

Gholamy, A., Kreinovich, V., Kosheleva, O., 2018. Why 70/30 or 80/20 Relation Between Training and Testing Sets: A Pedagogical Explanation. Dep. Tech. Rep. CS.

Goldberg, S., Glaubig, R.A., 1988. Boron and Silicon Adsorption on an Aluminum Oxide. *Soil Sci. Soc. Am. J.* **52**: 87–91.

Gong, H., Chen, K., Chen, G., Wang, S., Zhang, C., 2003. Effects of Silicon on Growth of Wheat Under Drought. *J. Plant Nutr.* **26**, 1055–1063.

Guntzer, F., Keller, C., Poulton, P.R., McGrath, S.P., Meunier, J.-D., 2012. Long-term removal of wheat straw decreases soil amorphous silica at Broadbalk, Rothamsted. *Plant Soil.* **352**: 173–184.

Harris, C.R., Millman, K.J., van der Walt, S.J., Gommers, R., Virtanen, P., Cournapeau, D., Wieser, E., Taylor, J., Berg, S., Smith, N.J., Kern, R., Picus, M., Hoyer, S., van Kerkwijk, M.H., Brett, M., Haldane, A., del Río, J.F., Wiebe, M., Peterson, P., Gérard-Marchant, P., Sheppard, K., Reddy, T., Weckesser, W., Abbasi, H., Gohlke, C., Oliphant, T.E., 2020. Array programming with NumPy. *Nature.* **585**: 357–362.

Haynes, R.J., 2014. A contemporary overview of silicon availability in agricultural soils. *J. Plant Nutr. Soil Sci.* **177**: 831–844.

Haynes, R.J., 2017. The nature of biogenic Si and its potential role in Si supply in agricultural soils. *Agric. Ecosyst. Environ.* **245**: 100–111.

Haynes, R.J., 2019. What effect does liming have on silicon availability in agricultural soils? *Geoderma* **337**: 375–383.

Haysom, M.B.C., Chapman, L.S., 1975. Some aspects of the calcium silicate trials at Mackay. *Proc Qls Soc Sug Cane Technol.* **42**: 17–22.

Hiebl, J., Frei, C., 2018. Daily precipitation grids for Austria since 1961—development and evaluation of a spatial dataset for hydroclimatic monitoring and modelling. *Theor. Appl. Climatol.* **132**: 327–345.

Hiemstra, T., Barnett, M.O., van Riemsdijk, W.H., 2007. Interaction of silicic acid with goethite. *J. Colloid Interface Sci.* **310**: 8–17.

Hodson, M.J., White, P.J., Mead, A., Broadley, M.R., 2005. Phylogenetic Variation in the Silicon Composition of Plants. *Ann. Bot.* **96**:1027–1046.

Huang, L., Parsons, C.T., Slowinski, S., Van Cappellen, P., 2022. Amorphous silica dissolution kinetics in freshwater environments: Effects of Fe2+ and other solution compositional controls. *Sci. Total Environ.* **851**:158239.

Hunter, J.D., 2007. Matplotlib: A 2D Graphics Environment. *Comput. Sci. Eng.* **9**: 90–95.

Iglesias, A., Garrote, L., 2015. Adaptation strategies for agricultural water management under climate change in Europe. *Agric. Water Manag.* **155**: 113–124.

IUSS Working Group WRB, 2022. World Reference Base for Soil Resources. International soil classification system for naming soils and creating legends for soil maps. fourth ed. International Union of Soil Sciences (IUSS), Vienna. https://www.isric.org/sites/default/files/WRB_fourth_edition_2022-12-18.pdf.

Johnson, S.N., Chen, Z.-H., Rowe, R.C., Tissue, D.T., 2022. Field application of silicon alleviates drought stress and improves water use efficiency in wheat. *Front. Plant Sci.* **13**.

Johnson, S.N., Ryalls, J.M.W., Gherlenda, A.N., Frew, A., Hartley, S.E., 2018. Benefits from Below: Silicon

Supplementation Maintains Legume Productivity under Predicted Climate Change Scenarios. *Front. Plant Sci.* **9**.
Jones, L.H.P., Handreck, K.A., 1963. Effects of Iron and Aluminium Oxides on Silica in Solution in Soils. *Nature.* **198**:852–853.
Jones, L.H.P., Handreck, K.A., 1967. Silica In Soils, Plants, and Animals, in: Advances in Agronomy. Elsevier, pp. 107–149.
Joseph, V.R., 2022. Optimal ratio for data splitting. *Stat. Anal. Data Min. ASA Data Sci. J.* **15**: 531–538.
Kaczorek, D., Puppe, D., Busse, J., Sommer, M., 2019. Effects of phytolith distribution and characteristics on extractable silicon fractions in soils under different vegetation – An exploratory study on loess. *Geoderma.* **356**: 113917.
Keeping, M.G., 2017. Uptake of Silicon by Sugarcane from Applied Sources May Not Reflect Plant-Available Soil Silicon and Total Silicon Content of Sources. *Front. Plant Sci.* **8**.
Keller, C., Guntzer, F., Barboni, D., Labreuche, J., Meunier, J.-D., 2012. Impact of agriculture on the Si biogeochemical cycle: Input from phytolith studies. *Comptes Rendus Geosci., Erosion–Alteration: from fundamental mechanisms to geodynamic consequences (Ebelmen's Symposium)* **344**: 739–746.
Keller, C., Rizwan, M., Meunier, J.-D., 2021. Are Clay Minerals a Significant Source of Si for Crops? A Comparison of Amorphous Silica and the Roles of the Mineral Type and pH. *Silicon.* **13**: 3611–3618.
Kursa, M.B., Rudnicki, W.R., 2010. Feature Selection with the Boruta Package. *J. Stat. Softw.* **36**: 1–13.
Landré, A., Cornu, S., Meunier, J.-D., Guerin, A., Arrouays, D., Caubet, M., Ratié, C., Saby, N.P.A., 2020. Do climate and land use affect the pool of total silicon concentration? A digital soil mapping approach of French topsoils. *Geoderma.* **364**: 114175.
Li, R., Gu, Z., Vachula, R.S., Dong, H., Xu, M., Chen, X., Xu, B., Sun, Y., 2024. Fire effects on phytolith carbon sequestration. *Sci. Rep.* **14**: 30009.
Loeppert, R.H., Inskeep, W.P., 1996. Iron, in: Bartels, J.M. (Ed.), Methods of soil analysis Part 3. Chemical methods. Soil Science Society of America, Inc; American Society of Agronomy Inc, Madison, Wisconsin, USA, pp. 639–664.
Lundberg, S., Lee, S.-I., 2017. A Unified Approach to Interpreting Model Predictions. *Proceedings of the 31st International Conference on Neural Information Processing Systems (NIPS'17)*. Curran Associated Inc., Red Hook, NY, USA, **4768-4777**.
Ma, J.F., Tamai, K., Yamaji, N., Mitani, N., Konishi, S., Katsuhara, M., Ishiguro, M., Murata, Y., Yano, M., 2006. A silicon transporter in rice. *Nature* **440**: 688–691.
Ma, J.F., Yamaji, N., 2006. Silicon uptake and accumulation in higher plants. *Trends Plant Sci.* **11**: 392–397.
Mayland, H.F., Wright, J.L., Sojka, R.E., 1991. Silicon accumulation and water uptake by wheat. *Plant Soil.* **137**: 191–199.
McKeague, J.A., Cline, M.G., 1963. Silica in soil solutions: ii. The adsorption of monosilicic acid by soil and by other substances. *Can. J. Soil Sci.* **43**: 83–96.
McKinney, W., 2010. Data Structures for Statistical Computing in Python. *Proc. 9th Python Sci. Conf.* 56–61.
Meirelles, G., Deus, A., Fernandes, D., Bull, L., 2022. Evaluation of Silicon Bioavailability in Soil with Different Chemical Extractants. *Silicon.* **15**.
Meunier, J.-D., Sandhya, K., Prakash, N.B., Borschneck, D., Dussouillez, P., 2018. pH as a proxy for estimating plant-available Si? A case study in rice fields in Karnataka (South India). *Plant Soil* **432**: 143–155.
Miles, N., Manson, A.D., Rhodes, R., van Antwerpen, R., Weigel, A., 2014. Extractable Silicon in Soils of the South African Sugar Industry and Relationships with Crop Uptake. *Commun. Soil Sci. Plant Anal.* **45**: 2949–2958.
Miyake, Y., Takahashi, E., 1978. Silicon deficiency of tomato plant. *Soil Sci. Plant Nutr.* **24**, 175–189.
Miyake, Y., Takahashi, E., 1985. Effect of Silicon on the Growth of Soybean Plants in a Solution Culture. *Soil Sci. Plant Nutr.* **31**: 625–636.
Monoshyn, D., Chibesa, M.C., Puschenreiter, M., Zaller, J.G., Santner, J., 2024. Impact of earthworms on soil Si availability and wheat Si concentration in low- and high-Si soils. *Appl. Soil Ecol.* **201**: 105483.
Morrison, IR, Wilson, AL (1963) The absorptiometric determination of silicon in water. Part II. Method for determining "reactive" silicon in power-station waters. *Analyst.* **88**: 100–104.
Nanayakkara, U.N., Uddin, W., Datnoff, L.E., 2008. Application of silicon sources increases silicon accumulation in perennial ryegrass turf on two soil types. *Plant Soil.* **303**: 83–94.
Narayanaswamy, C., Prakash, N.B., 2009. Calibration and Categorization of Plant Available Silicon in Rice Soils of South India. *J. Plant Nutr.* **32**: 1237–1254.
Nguyen, M.N., Dultz, S., Picardal, F., Bui, A.T.K., Pham, Q.V., Dam, T.T.N., Nguyen, C.X., Nguyen, N.T., Bui, H.T., 2016. Simulation of silicon leaching from flooded rice paddy soils in the Red River Delta, Vietnam. *Chemosphere.* **145**: 450–456.

ÖNORM L 1080, 2013. Chemical soil analysis - Determination of organic carbon by dry combustion with and without consideration of carbonates (In German). Austrian Standards Institute, Wien.

ÖNORM L 1084, 1989. Chemical soil analyses - Determination of carbonate (In German). Österreichisches Normungsinstitut, Wien.

Pedregosa, F., Varoquaux, G., Gramfort, A., Michel, V., Thirion, B., Grisel, O., Blondel, M., Prettenhofer, P., Weiss, R., Dubourg, V., Vanderplas, J., Passos, A., Cournapeau, D., Brucher, M., Perrot, M., Duchesnay, É., 2011. Scikit-learn: Machine Learning in Python. *J. Mach. Learn. Res.* **12**: 2825–2830.

Puppe, D., Höhn, A., Kaczorek, D., Wanner, M., Wehrhan, M., Sommer, M., 2017. How big is the influence of biogenic silicon pools on short-term changes in water-soluble silicon in soils? Implications from a study of a 10-year-old soil–plant system. *Biogeosciences.* **14**: 5239–5252.

Puppe, D., Kaczorek, D., Schaller, J., Barkusky, D., Sommer, M., 2021. Crop straw recycling prevents anthropogenic desilication of agricultural soil–plant systems in the temperate zone – Results from a long-term field experiment in NE Germany. *Geoderma.* **403**: 115187.

Quigley, K., Donati, G., Anderson, T., 2017. Variation in the soil 'silicon landscape' explains plant silica accumulation across environmental gradients in Serengeti. *Plant Soil.* **410**.

Saccone, L., Conley, D.J., Koning, E., Sauer, D., Sommer, M., Kaczorek, D., Blecker, S.W., Kelly, E.F., 2007. Assessing the extraction and quantification of amorphous silica in soils of forest and grassland ecosystems. *Eur. J. Soil Sci.* **58**: 1446–1459.

Sangster, A.G., Hodson, M.J., 2007. Silica in Higher Plants, in: Ciba Foundation Symposium 121 - Silicon Biochemistry. John Wiley & Sons, Ltd, pp. 90–111.

Sauer, D., Saccone, L., Conley, D.J., Herrmann, L., Sommer, M., 2006. Review of methodologies for extracting plant-available and amorphous Si from soils and aquatic sediments. *Biogeochemistry* **80**: 89–108.

Saussure, Théod. de, 1804. Chemical research on vegetation. (In French). Nyon, Paris.

Savant, N., Korndörfer, G., Datnoff, L., Snyderc, G., 1999. Silicon nutrition and sugarcane production: A review. *J. Plant Nutr. - J PLANT NUTR.* **22**: 1853–1903.

Savant, N.K., Datnoff, L.E., Snyder, G.H., 1997. Depletion of plant-available silicon in soils: A possible cause of declining rice yields. *Commun. Soil Sci. Plant Anal.* **28**: 1245–1252.

Schaller, J., Turner, B.L., Weissflog, A., Pino, D., Bielnicka, A.W., Engelbrecht, B.M.J., 2018. Silicon in tropical forests: large variation across soils and leaves suggests ecological significance. *Biogeochemistry*. **140**: 161–174.

Sharma, R., Kumar, V., Kumar, R., 2019. Distribution of phytoliths in plants: a review. *Geol. Ecol. Landsc.* **3**: 123–148.

Singh, P., Kumar, V., Sharma, J., Saini, S., Sharma, P., Kumar, S., Sinhmar, Y., Kumar, D., Sharma, A., 2022. Silicon Supplementation Alleviates the Salinity Stress in Wheat Plants by Enhancing the Plant Water Status, Photosynthetic Pigments, Proline Content and Antioxidant Enzyme Activities. *Plants.* **11**, 2525.

Smis, A., Van Damme, S., Struyf, E., Clymans, W., Van Wesemael, B., Frot, E., Vandevenne, F., Van Hoestenberghe, T., Govers, G., Meire, P., 2011. A trade-off between dissolved and amorphous silica transport during peak flow events (Scheldt river basin, Belgium): impacts of precipitation intensity on terrestrial Si dynamics in strongly cultivated catchments. *Biogeochemistry*. **106**: 475–487.

Sommer, M., Kaczorek, D., Kuzyakov, Y., Breuer, J., 2006. Silicon pools and fluxes in soils and landscapes—a review. *J. Plant Nutr. Soil Sci.* **169**: 582–582.

Stein, M., Puppe, D., Kaczorek, D., Buhtz, C., Schaller, J., 2024. Silicon extraction from x-ray amorphous soil constituents: a method comparison of alkaline extracting agents. *Front. Environ. Sci.* **12**.

Struyf, E., Opdekamp, W., Backx, H., Jacobs, S., Conley, D.J., Meire, P., 2009. Vegetation and proximity to the river control amorphous silica storage in a riparian wetland (Biebrza National Park, Poland). *Biogeosciences.* **6**: 623–631.

Van Tol, J.J., Barnard, J., Rensburg, L., Le Roux, P., 2013. Soil depth inferred from electromagnetic induction measurements. *Afr. J. Agric. Res.* 519–524.

Vandevenne, F.I., Barão, L., Ronchi, B., Govers, G., Meire, P., Kelly, E.F., Struyf, E., 2015. Silicon pools in human impacted soils of temperate zones. *Glob. Biogeochem. Cycles.* **29**: 1439–1450.

Virtanen, P., Gommers, R., Oliphant, T.E., Haberland, M., Reddy, T., Cournapeau, D., Burovski, E., Peterson, P., Weckesser, W., Bright, J., van der Walt, S.J., Brett, M., Wilson, J., Millman, K.J., Mayorov, N., Nelson, A.R.J., Jones, E., Kern, R., Larson, E., Carey, C.J., Polat, İ., Feng, Y., Moore, E.W., VanderPlas, J., Laxalde, D., Perktold, J., Cimrman, R., Henriksen, I., Quintero, E.A., Harris, C.R., Archibald, A.M., Ribeiro, A.H., Pedregosa, F., van Mulbregt, P., 2020. SciPy 1.0: fundamental algorithms for scientific computing in Python. *Nat. Methods*. **17**: 261–272.

Walsh, O.S., Shafian, S., McClintick-Chess, J.R., Belmont, K.M., Blanscet, S.M., 2018. Potential of Silicon Amendment for Improved Wheat Production. *Plants.* **7**: 26.

Wenzel, W.W., Duboc, O., Golestanifard, A., Holzinger, C., Mayr, K., Reiter, J., Schiefer, A., 2022. Soil and land use factors control organic carbon status and accumulation in agricultural soils of Lower Austria. *Geoderma.* **409**: 115595.

Wenzel, W.W., Philipsen, F.N., Herold, L., Kingsland-Mengi, A., Laux, M., Golestanifard, A., Strobel, B.W., Duboc, O., 2023. Carbon sequestration potential and fractionation in soils after conversion of cultivated land to hedgerows, *Geoderma.* **435**: 116501.

Wu, J., Geilfus, C.-M., Pitann, B., Mühling, K.-H., 2016. Silicon-enhanced oxalate exudation contributes to alleviation of cadmium toxicity in wheat. *Environ. Exp. Bot.* **131**: 10–18.

Xie, C., Antić, N., Nadal-Romero, E., Yan, L., Tosti, T., Djogo Mračević, S., Tu, X., Kašanin-Grubin, M., 2022. The Influences of Climatic and Lithological Factors on Weathering of Sediments in Humid Badland Areas. *Front. Earth Sci.* **10**.

Yanai, J., Taniguchi, H., Nakao, A., 2016. Evaluation of available silicon content and its determining factors of agricultural soils in Japan. *Soil Sci. Plant Nutr.* **62**: 511–518.

Yang, S., Hao, Q., Liu, H., Zhang, X., Yu, C., Yang, X., Xia, S., Yang, W., Li, J., Song, Z., 2019. Impact of grassland degradation on the distribution and bioavailability of soil silicon: Implications for the Si cycle in grasslands. *Sci. Total Environ.* **657**: 811–818.

Yang, X., Song, Z., Van Zwieten, L., Sun, X., Yu, C., Wang, W., Liu, C., Wang, H., 2021. Spatial distribution of plant-available silicon and its controlling factors in paddy fields of China. *Geoderma.* **401**: 115215.

# Supplementary Information

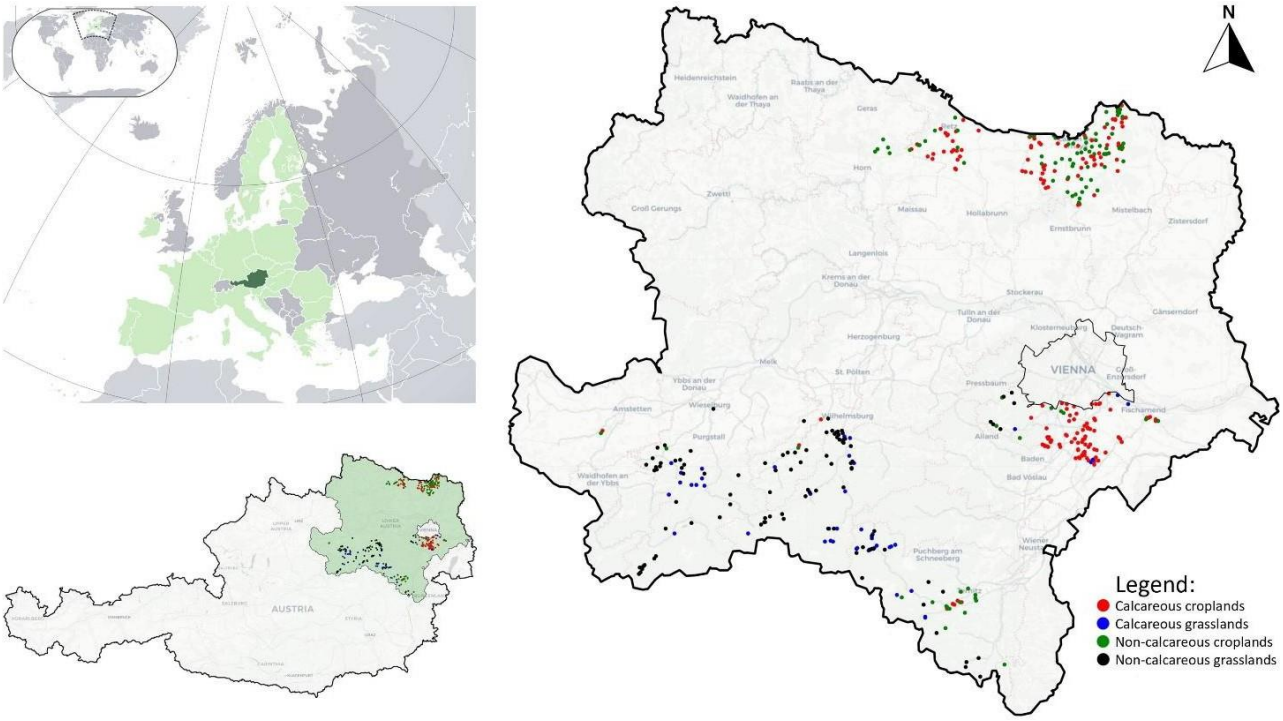


**Figure S1.** Map of sampling locations around Lower Austria. The map was prepared using data from Sevdari & Marmullaku (2023), Wikimedia Commons, and the Amt der Niederösterreichischen Landesregierung Open Government Data API.

Figure References:

Sevdari, Kristian; Marmullaku, Drin (2023). Shapefile of European countries. Technical University of Denmark. Dataset. https://doi.org/10.11583/DTU.23686383

Wikimedia Commons. (n.d.). EU-Austria (orthographic projection) [SVG image]. Retrieved February 21, 2025, from https://commons.wikimedia.org/wiki/File:EU-Austria_(orthographic_projection).svg

Amt der Niederösterreichischen Landesregierung. (n.d.). Schnittstelle API – Open Government Data Niederösterreich. Retrieved September 24, 2024, from https://www.noe.gv.at/noe/Open-Government-Data/Schnittstelle_API.html

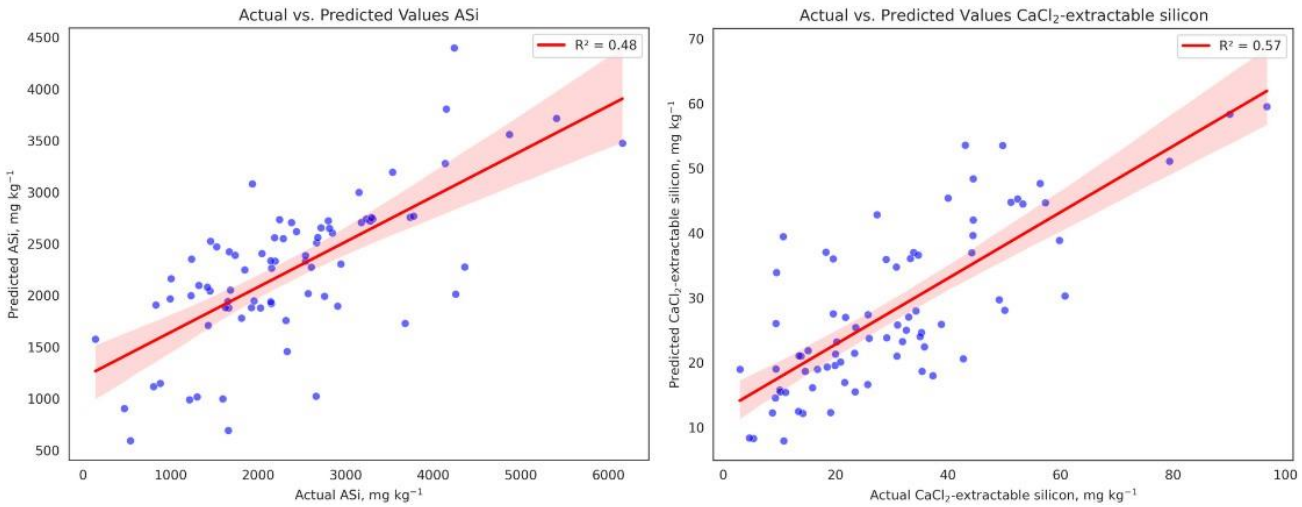


**Figure S2.** Regression plots and corresponding $r^2$ values for the basic models. The red shaded area represents the standard error. These models are shown prior to cross-validation.

**Table S1.** Analyzed soil variables and their use for particular evaluation steps. IS - Initial Sampling, RS - Resampling.

| ***Variable*** | ***Dataset*** | |
|---|---|---|
| | **IS** | **RS** |
| | *Measured in sample set* | |
| $Si_{CaCl2}$ | x | x |
| ASi | x | x |
| pH | x | x |
| $CaCO_3$ content | x | x |
| Fe oxy-hydroxides | x | |
| Al oxy-hydroxides | x | |
| Soil texture | x | |
| SOC | x | x |
| | *Used in data evaluation* | |
| Random forest analysis | x | |
| Analysis of changes due to altered management practices | x | x |